

DRAG COEFFICIENTS FOR FLAT SQUARE PLATES
OSCILLATING NORMAL TO THEIR PLANES--IN AIR

By William E. Woolam

Distribution of this report is provided in the interest of information exchange. Responsibility for the contents resides in the author or organization that prepared it.

Issued by Originator as Final Report, Project 02-1973

Prepared under Contract No. NAS1-6659 by
SOUTHWEST RESEARCH INSTITUTE
San Antonio, Texas

for Langley Research Center

NATIONAL AERONAUTICAL AND SPACE ADMINISTRATION



TABLE OF CONTENTS

	<u>Page</u>
ABSTRACT	1
INTRODUCTION	1
SYMBOLS	2
DIMENSIONAL ANALYSIS	4
OSCILLATORY DRAG COEFFICIENTS "STATE-OF-THE-ART"	5
Reynolds Number	5
Period Parameter	6
Frequency	10
Thickness	12
Area	12
APPARATUS AND TEST PROCEDURE	12
The Free-Decay Method	12
The Forced Vibration Method	18
ANALYSIS	24
Free-Decay Method	24
Forced Vibration Method	28
DISCUSSION OF THE RESULTS	31
Amplitude	31
Frequency	36
Thickness	36
Area	36
Virtual Mass	40
ENGINEERING APPLICATION OF OSCILLATORY DRAG COEFFICIENTS	42
CONCLUSIONS	45
REFERENCES	46

PRECEDING PAGE BLANK NOT FILMED.

LIST OF ILLUSTRATIONS

<u>Figure</u>		<u>Page</u>
1	Oscillatory Drag Coefficient vs Reynolds Number as Measured by Kuelegan and Carpenter (Ref. 4)	7
2	Steady State Drag Coefficients of Circular and Square Plates as a Function of Reynolds Number (Ref. 7)	8
3	Drag Coefficient vs Period Parameter for Flow Normal to a Flat Plate (Ref. 4)	9
4	Drag Coefficient vs Period Parameter with Variation of Aspect Ratio (Ref. 5)	11
5	Front View of Free-Decay Test Apparatus	13
6	Free Decay of a $20 \times 20 \times 0.16$ -In. Plate	14
7	Large Amplitude Horizontal Oscillator	19
8	Panel in Horizontal Position for Inertia Cancellation	20
9	Dynamometer Used for Drag Force Measurements	22
10	Dynamometer Used for Inertia Cancellation	23
11	Drag Forces Measured on a $20 \times 20 \times 0.32$ -In. Plate Oscillated at an Amplitude of 4 In. 0-Pk and a Frequency of 2 Hz	25
12	Plate Oscillator Schematic	26
13	Theoretically Calculated Drag, Inertial, and Total Forces for a $20 \times 20 \times 0.32$ -In. Plate	30
14a	Drag Coefficient for the $10 \times 10 \times 0.16$ -In. Plate at an Oscillatory Frequency of 0.63 Hz	32
14b	Air Damping for a $10 \times 10 \times 0.16$ -In. Plate Obtained by the Free-Decay Method	32
15a	Drag Coefficient for the $20 \times 20 \times 0.32$ -In. Plate at an Oscillatory Frequency of 0.63 Hz	33
15b	Air Damping for a $20 \times 20 \times 0.32$ -In. Plate Obtained by the Free-Decay Method	33

LIST OF ILLUSTRATIONS (Cont'd)

<u>Figure</u>		<u>Page</u>
16a	Drag Coefficient for the $40 \times 40 \times 0.64$ -In. Plate at an Oscillatory Frequency of 0.63 Hz	34
16b	Air Damping for a $40 \times 40 \times 0.64$ -In. Plate Obtained by the Free-Decay Method	34
17	Summary of Oscillatory Drag Coefficient for Five Different Plates at 0.63 Hz	35
18a	Air Damping of a $20 \times 20 \times 0.32$ -In. Plate with a Frequency Variation	37
18b	Damping of a $20 \times 20 \times 0.32$ -In. Plate Obtained by Free-Decay Method	37
19	Drag Coefficients at Varying Period Parameters and Frequencies Obtained by Forced Vibration Method	38
20	Drag Coefficients at Varying Period Parameters and Frequencies Obtained by Forced Vibration Method	39
21	Variation of the Drag Coefficient as a Function of Plate Area	41
22	Virtual Mass Coefficients Obtained from Free-Decay Period Changes	43

DRAG COEFFICIENTS FOR FLAT SQUARE PLATES OSCILLATING NORMALLY TO THEIR PLANES--IN AIR

By William E. Woolam
Southwest Research Institute

ABSTRACT

An investigation was conducted to determine the drag coefficients for flat plates oscillating normal to their planes. With this specific objective in mind, a dimensional analysis was performed from which several dimensionless parameters were chosen for a detailed experimental study. These parameters include amplitude of oscillation, frequency of oscillation, plate thickness, and area. The present study indicates that the oscillatory drag coefficient is a function of the plate area to the four-thirds power, which is in agreement with earlier investigations by Stephens and Scavullo. There is evidence that over a frequency range of 0.48 to 21.2 Hz, the oscillatory drag coefficients are independent of the frequency of the plate oscillation. Within the range of parameters considered, there appears to be an indistinguishable effect of both the plate thickness and the amplitude of oscillation on the oscillatory drag coefficient.

INTRODUCTION

It is often necessary to predict the vibration analysis of lightweight, large surface area panels such as solar panels or long satellite antennae. Without a proper understanding of the air damping mechanisms, it would be necessary to conduct full-scale vibration tests in a large vacuum chamber; however, this is both costly and time-consuming. If the drag as a result of unsteady flow is sufficiently understood, then the following analytical or experimental possibilities exist:

- (1) Providing the structural damping can be predicted accurately and the structural properties of the solar panel or antennae are available, it is possible to analytically calculate the vibratory response of the panels or antennae or if these properties are not known, then,
- (2) The vibration tests could be conducted in-air and the results extrapolated to an in-vacuo environment and, in addition,
- (3) It would provide a method of designing vacuum tests in order to sufficiently minimize the air damping; e. g., there has been

discussion concerning the pressure level necessary to perform vibration tests on a model and maintain model similitude.

Drag coefficients for flat plates under unsteady or oscillatory flow conditions have been shown by several investigators to be larger than for steady flow conditions and also a function of the amplitude of oscillation, often called the period parameter (Refs. 1-6). Up until the present time, most of the concern has been with heavy density liquids, normally water, and, in many cases, the panels are rigid. The present research was conducted in order to determine the oscillatory drag coefficients of a rigid panel oscillating in air. In the present report, an extension of the rigid panel data to a flexible cantilever panel is demonstrated. Based on studies of the full-scale or model solar panel vibration characteristics under atmospheric laboratory conditions, it would then be possible to predict the solar panel* vibration amplitudes in an outer space environment.

SYMBOLS

A	beam tip amplitude
A_n	beam tip amplitude for the n-th mode
b	plate width
C_d	drag coefficient for steady flow
\tilde{C}_d	drag coefficient for oscillatory flow
$\tilde{C}_d(x, t)$	drag coefficient for oscillatory flow; a function of amplitude and time
\tilde{C}_m	mass coefficient for oscillatory flow; a function of amplitude and time
F	force
\tilde{F}_d	drag force for a given amplitude for oscillatory flow conditions
$\tilde{F}_d(t)$	oscillatory time varying drag force
f_p	frequency of oscillation for the plate
f_v	vortex shedding frequency
$f_v b / V_p$	Strouhal number
h	plate thickness
k_e	equivalent spring rate of the combined pendulum and flexural spring system

*Throughout the remainder of the text, the term plate will be used instead of panel in order to coincide with the terminology of the various references.

l	length of the plate
M	bending moment
m	the calibration mass used in the forced vibration test
m_b	the total mass of the cantilever beam
m_e	equivalent mass of the oscillatory system
m_s	mass of the structure
m_v	virtual mass
N	number of complete cycles of oscillation
n	modal number
R	Reynolds number, equivalent to $U_m b / \nu$
S	plate area; all plates are square; therefore, $S = b^2$
t	time
U_m	maximum velocity
$\frac{U_m \tau}{b}$	period parameter
V	velocity
V_p	plate velocity
x	amplitude
\dot{x}	velocity
\ddot{x}	acceleration
x_0	amplitude of plate oscillation measured from zero to peak
$\frac{x_0}{b}$	period parameter; equivalent to $\left(\frac{U_m \tau}{b}\right) / 2\pi$
β_n	mode shape contributing factor
δ_a	the logarithmic decrement as a result of air damping alone
$\delta_a + s$	the logarithmic decrement as a result of both air damping and structural damping
δ_s	the logarithmic decrement as a result of structural damping alone
μ_a	viscosity of air

ν	kinematic viscosity of air
ρ	beam density
ρ_a	mass density of air, $1.085 \times 10^{-7} \frac{\text{lb sec}^2}{\text{in}^4}$
ρ_p	plate density
τ	period for oscillating plate
τ_h	period for plate in horizontal condition
τ_v	period for plate in vertical condition
Φ	normal mode function
ω	radial frequency
$\frac{\partial}{\partial t}$	partial differentiation with respect to the time coordinate
$\frac{\partial}{\partial x}$	partial differentiation with respect to the spatial coordinate

DIMENSIONAL ANALYSIS

The following variables may, at least intuitively, affect the air damping phenomenon for a plate oscillating normal to its plane:

	<u>Variables</u>	<u>Symbol</u>	<u>Dimension</u>
<u>Plate</u>	Width	b	L
	Area	$S = bl$	L^2
	Thickness	h	L
	Density	ρ_p	FT^2/L^4
<u>Air</u>	Density	ρ_a	FT^2/L^4
	Viscosity	μ_a	FT/L^2
<u>Dynamics</u>	Displacement	x	L
	Velocity	V	L/T
	Vibration Frequency of a Rigid Panel	$f_p = \omega/2\pi$	$1/T$
	Time	t	T
	Force	F	F
	Vortex Frequency	f_v	$1/T$

From these variables, the following set of independent dimensionless π terms were derived:

<u>No.</u>	<u>Term</u>	<u>Description</u>
π_1	b/h	Width to thickness ratio
π_2	x/b	Displacement to width ratio
π_3	S/h^2	Area to thickness squared ratio
π_4	ρ_a / ρ_p	Density ratio
π_5	Vb/ν	Reynolds number
π_6	$f_v b/V$	Strouhal number
π_7	$F/S\rho_a V^2$	Drag coefficient
π_8	$f_p t$	Scaled time

The first three π terms are related to the plate geometry and the amplitude of oscillation. The π_2 term can be shown to be the "period parameter" used by several investigators. The π_4 term is related to the virtual mass effects, π_5 to the viscous effects, π_6 to the vortex shedding, π_7 to pressure drag (commonly recognized as the drag coefficient, C_D), and π_8 serves to interpret the test results. Other test parameters which are considered worthy of future studies are the influence of the plate perimeter on the drag, the geometric effect on the drag coefficient, and variation of the oscillatory drag coefficient with the change of the aspect ratio.

It is interesting to examine the "state-of-the-art" (Refs. 1-6) in some of these areas which were considered to be of primary interest.

OSCILLATORY DRAG COEFFICIENTS "STATE-OF-THE-ART"

The following paragraphs outline parameters which might affect the oscillatory drag on a flat plate and discuss their relation to the present "state-of-the-art."

Reynolds Number

Kuelegan and Carpenter (Ref. 4) presented a remarkable paper in 1958 which discussed in great detail the hydrodynamic drag and inertial forces experienced by cylinders and plates in an oscillating fluid. Drag coefficients experienced by flat plates for certain conditions were several times larger than those characteristic of steady flow conditions. As a result of their studies, they concluded that there is no meaningful correlation

between the oscillatory drag coefficient \tilde{C}_D^* and the Reynolds number (see Figure 1). It is interesting to note that using Kuelegan and Carpenter's definition of Reynolds number, i. e., based on peak vibration, all of the tests appear to have been conducted at Reynolds numbers above the viscous flow regime which begins at $R = 100$. Below $R = 100$, the steady flow drag mechanism is of a viscous nature, whereas, above $R = 100$, the drag mechanism is primarily turbulent (Ref. 7). If instead the Reynolds number for oscillatory flow is defined using the instantaneous velocity, then the Reynolds number will vary from zero to a finite value since the velocity of the plate or airstream varies from zero to a finite value. The crosshatched area in Figure 2 illustrates, on a steady flow "drag coefficient versus Reynolds number" curve, the Reynolds number regime which the Kuelegan and Carpenter tests covered, based on instantaneous velocities. It might even be suspected that the viscous flow portion of the oscillation might contribute a substantial drag force to cause the overall drag coefficient to be larger than would be insinuated if a Reynolds number is used based on the peak velocity. These points are mentioned in order that the reader will not place undue emphasis on the complete absence of Reynolds number effects. It is difficult, however, to extend the Reynolds number definition to a non-steady flow problem.

Period Parameter

The studies conducted by Kuelegan and Carpenter did reveal that instead of a Reynolds number correlation, there is a correlation between the oscillatory drag coefficient and a parameter which they defined as the "period parameter" (Fig. 3). These two investigators felt certain that the primary mechanism which altered the oscillatory drag coefficients was the process of eddy shedding. Kuelegan and Carpenter defined the "period parameter" as $\frac{U_m \tau}{b}$, or, by substituting $U_m = 2\pi f x_0$ and $\tau = \frac{1}{f}$ into this relationship, the "period parameter" = $2\pi \frac{x_0}{b}$. This relationship indicates that the oscillatory drag coefficient is not a function of the frequency. The frequency was not varied in any of the Kuelegan and Carpenter experiments even though the Reynolds number was varied from $R = 4,500$ to $12,800$. The oscillatory drag forces were obtained by producing a uniform sinusoidal water current over the plates. The resulting forces on the plates were recorded, and a Fourier analysis method was used to separate the pressure drag forces and liquid inertial forces. Kuelegan and Carpenter used plates which extended from one side of the channel to the other in an effort to approximate as closely as possible the condition of an infinite aspect ratio.

*Throughout the text of this report, \tilde{C}_D will be used to identify the oscillatory drag coefficient as compared to C_D for the steady flow drag coefficient.

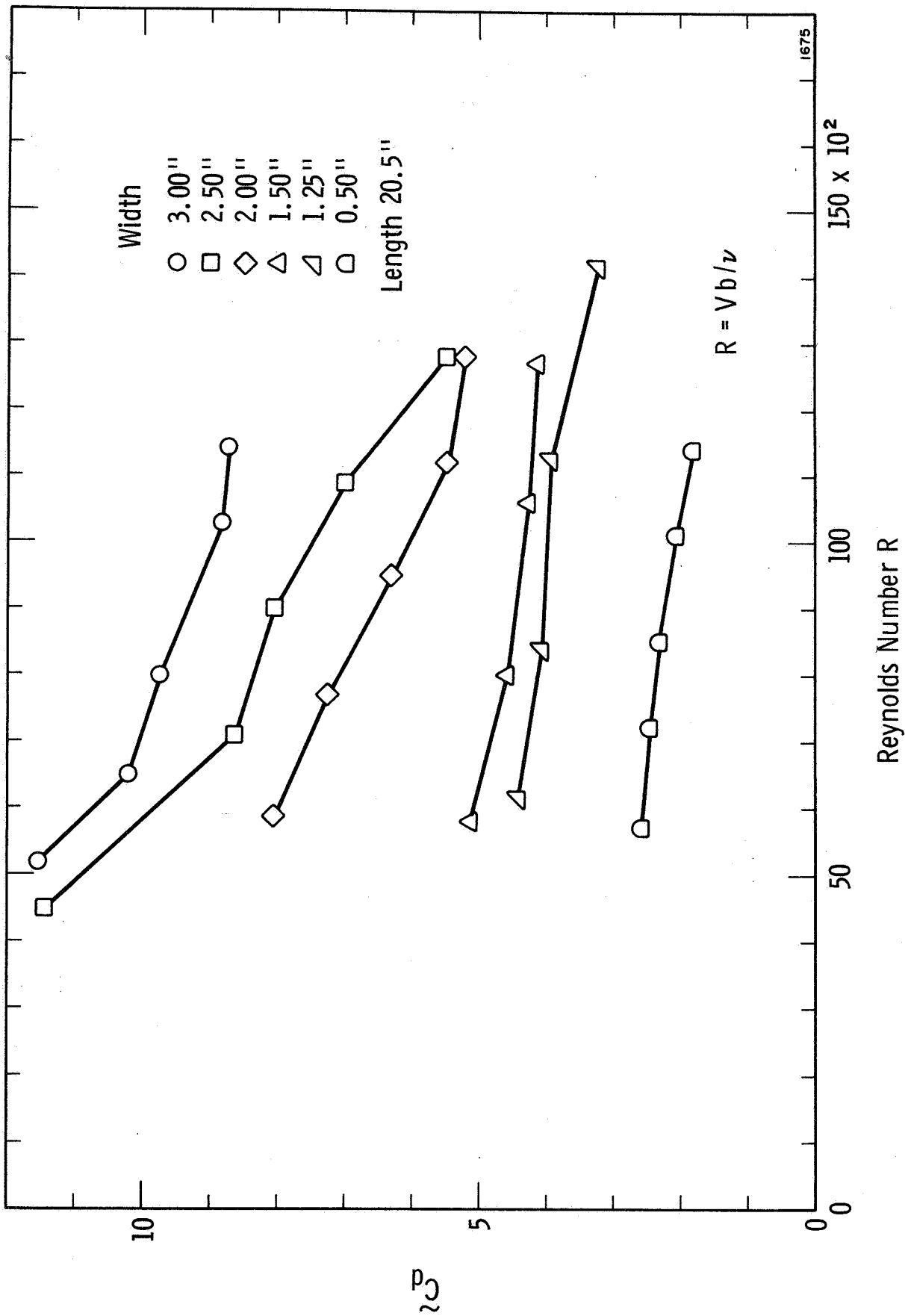


FIGURE 1. OSCILLATORY DRAG COEFFICIENT VS REYNOLDS NUMBER AS MEASURED BY KUELEGAN AND CARPENTER (Ref. 4)

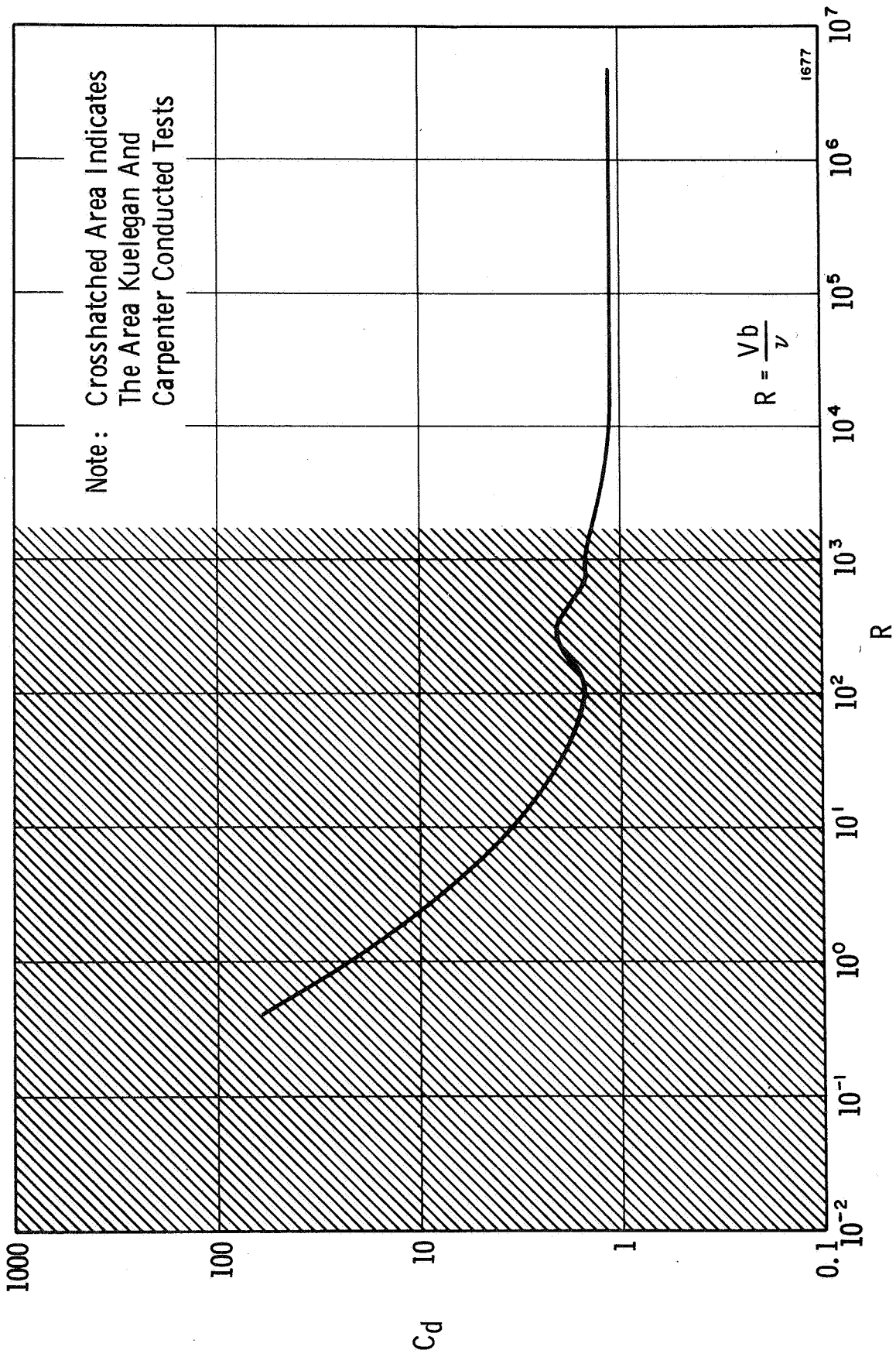


FIGURE 2. STEADY STATE DRAG COEFFICIENTS OF CIRCULAR AND SQUARE PLATES AS A FUNCTION OF REYNOLDS NUMBER (Ref. 7)

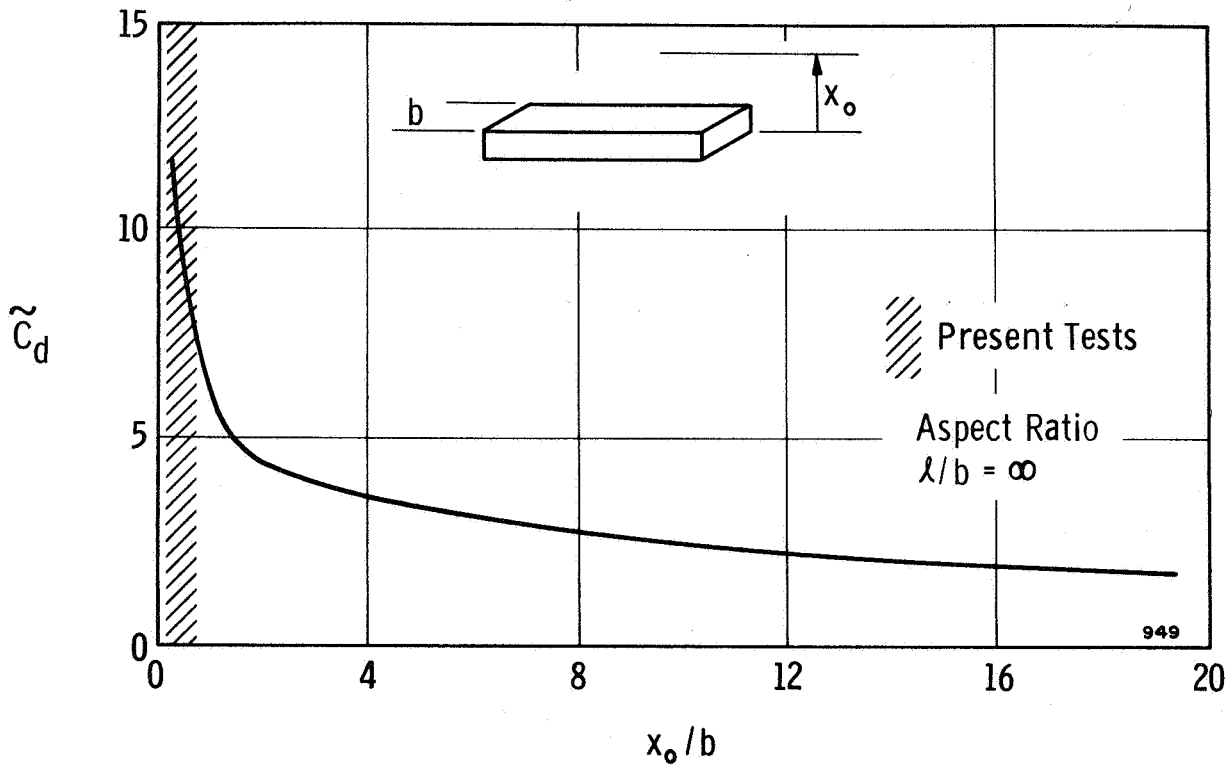


FIGURE 3. DRAG COEFFICIENT VS PERIOD PARAMETER FOR FLOW NORMAL TO A FLAT PLATE (Ref. 4)

Following the work by Kuelegan and Carpenter, additional experimental results were obtained by Martin (Ref. 5) and Ridjanovic (Ref. 6). Martin investigated the case of a plate with an infinite aspect ratio, i.e., the case of two-dimensional flow. Ridjanovic later extended this study in order to determine the effect of aspect ratio (see Fig. 4) on the oscillatory drag coefficients. Both Ridjanovic and Martin used a free-decay method for obtaining the oscillatory drag coefficients, similar to the method which has been used in this report.

The initial interest in the oscillatory drag coefficients was with respect to wave-induced forces on vertical pilings and submerged objects typical of offshore platforms. The studies conducted by Kuelegan and Carpenter were primarily of a basic research nature stimulated by these earlier interests. The works performed by Martin and Ridjanovic were related to the roll damping properties provided by ship bilge keels which are attached to the hull of a ship for the purpose of providing an additional hydrodynamic damping effect. More recently, the concept of oscillatory drag coefficients has been extended to the damping provided by flexible baffles used in liquid propellant launch vehicles for the suppression of a phenomenon known as "liquid sloshing" (Refs. 8 and 9).

The general consensus of all the investigators is that the large values of oscillatory drag coefficients which have been observed are a result of starting but not fully formed wakes or fully developed vortices. It appears that the big gap left in "the-state-of-the-art" is in the area of theoretically predicting the high values of oscillatory drag coefficients by consideration of the discrete vortices which are shed from the edges of the plate. In an effort to make the theoretical problem tractable, it is necessary to assume a two-dimensional, incompressible, irrotational flow. Then, knowing the relative velocity between the vortices and the oscillating plate combined with the knowledge of the vortex spacing, it might be possible to obtain, at the best, a semitheoretical solution--semitheoretical because energy in fluids can be dissipated only through a viscous flow model and, therefore, the rigorous application of an irrotational model is not meaningful. It might be possible, however, to use the irrotational model and experimental results to provide the input parameters.

Frequency

Specific tests have not been conducted yet to determine the effects of frequency on the oscillatory drag coefficient. According to the results of previous investigations, the drag coefficient is not frequency dependent; however, the dimensional analysis suggests the possible importance of the Strouhal number effect. Tests were conducted on the same plate size at three different frequencies in order to determine the Strouhal number effect on the oscillatory drag coefficients.

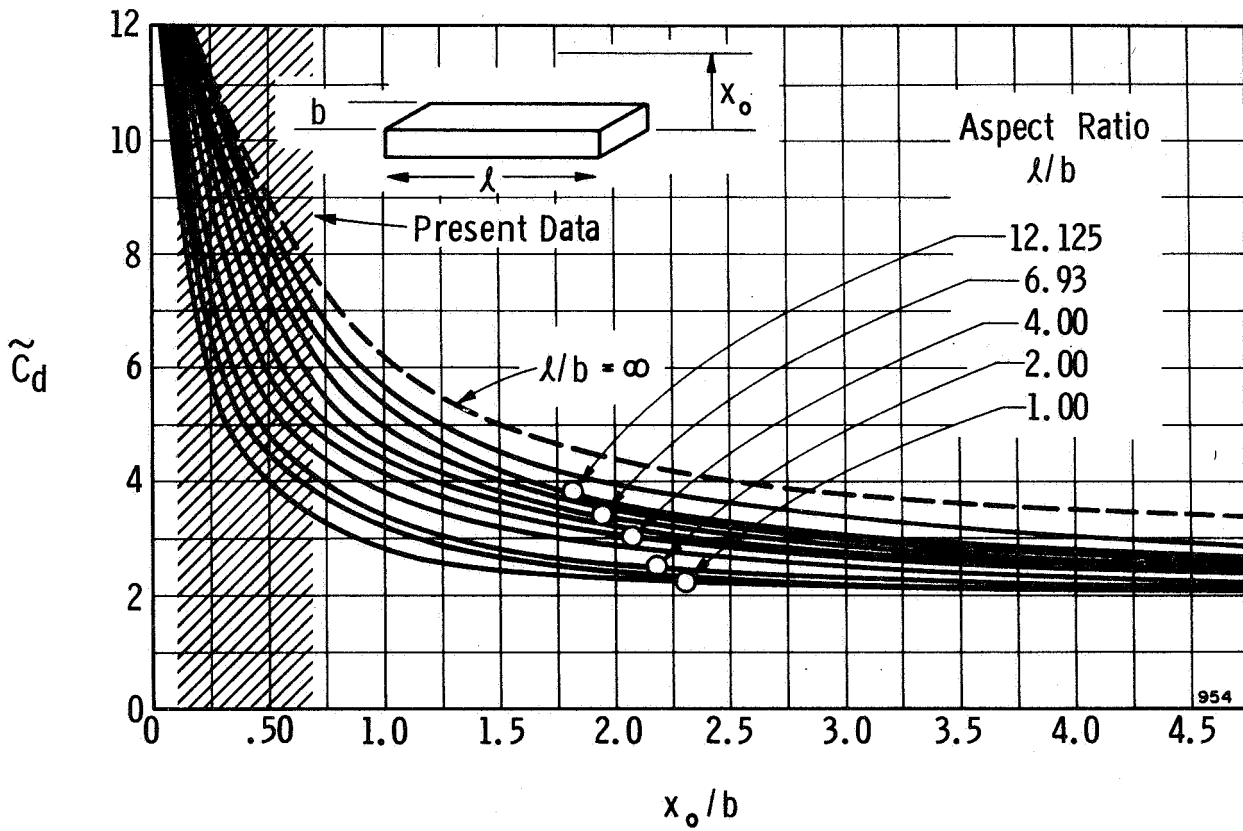


FIGURE 4. DRAG COEFFICIENT VS PERIOD PARAMETER WITH VARIATION OF ASPECT RATIO (Ref. 5)

Thickness

In the tests conducted by both Kuelegan and Carpenter, and Ridjanovic, the thickness of the plate was constant. The panels tested in the present report were geometrically scaled; i. e., the width to thickness ratio was constant except where the thickness effect was of primary interest. In order to determine the thickness effect, thin aluminum edges were placed on these same plates to provide more than an order of magnitude reduction in the width/thickness ratio, the purpose being to observe detectable changes in the oscillatory drag coefficients.

Area

Investigations by Stephens and Scavullo (Ref. 2) indicate that the oscillatory drag coefficients for flat plates vary with the four-thirds power of the area. In the present set of tests, plates of 100-, 400-, and 1600-sq in. surface area were used to determine the effect of the plate area on the oscillatory drag coefficients.

The primary purpose of the present study is to determine the air damping mechanisms which act on a large oscillating plate and determine the parameters which affect these mechanisms. Then, by a mathematical representation of the air damping forces in an equation of motion, one can predict the vibration response of a plate for an in-vacuo condition, based on the response data obtained from in-air tests. It might be conceivable, with a better knowledge of the structural damping mechanisms, that the response of a large surface area plate can be predicted analytically without the requirements of full-scale tests.

APPARATUS AND TEST PROCEDURE

Two test methods were used to obtain data from which the oscillatory drag coefficients were calculated: (1) a free-decay method, and (2) a forced vibration method. In the following paragraphs, these two methods are discussed in detail.

The Free-Decay Method

The free-decay method is the simplest of the two techniques and requires the least amount of instrumentation. Figure 5 illustrates the test apparatus used for the free-decay tests, while Figure 6 illustrates typical data which were obtained during test runs of the $20 \times 20 \times 0.32$ -in. plate. The test apparatus consists of a parallelogram type spring-loaded pendulum. The parallelogram type design was used in order to oscillate the plate in a

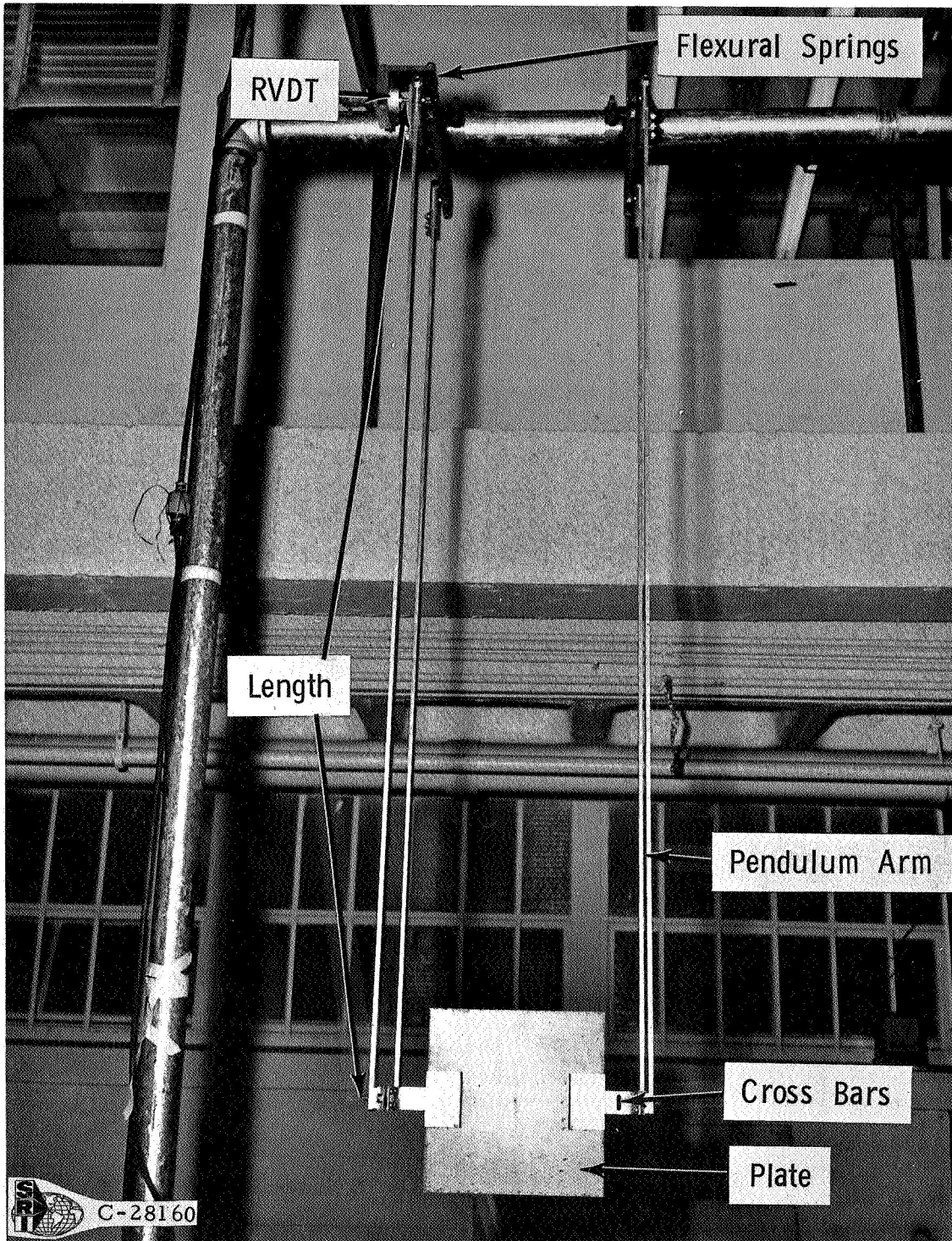


FIGURE 5. FRONT VIEW OF FREE-DECAY TEST APPARATUS

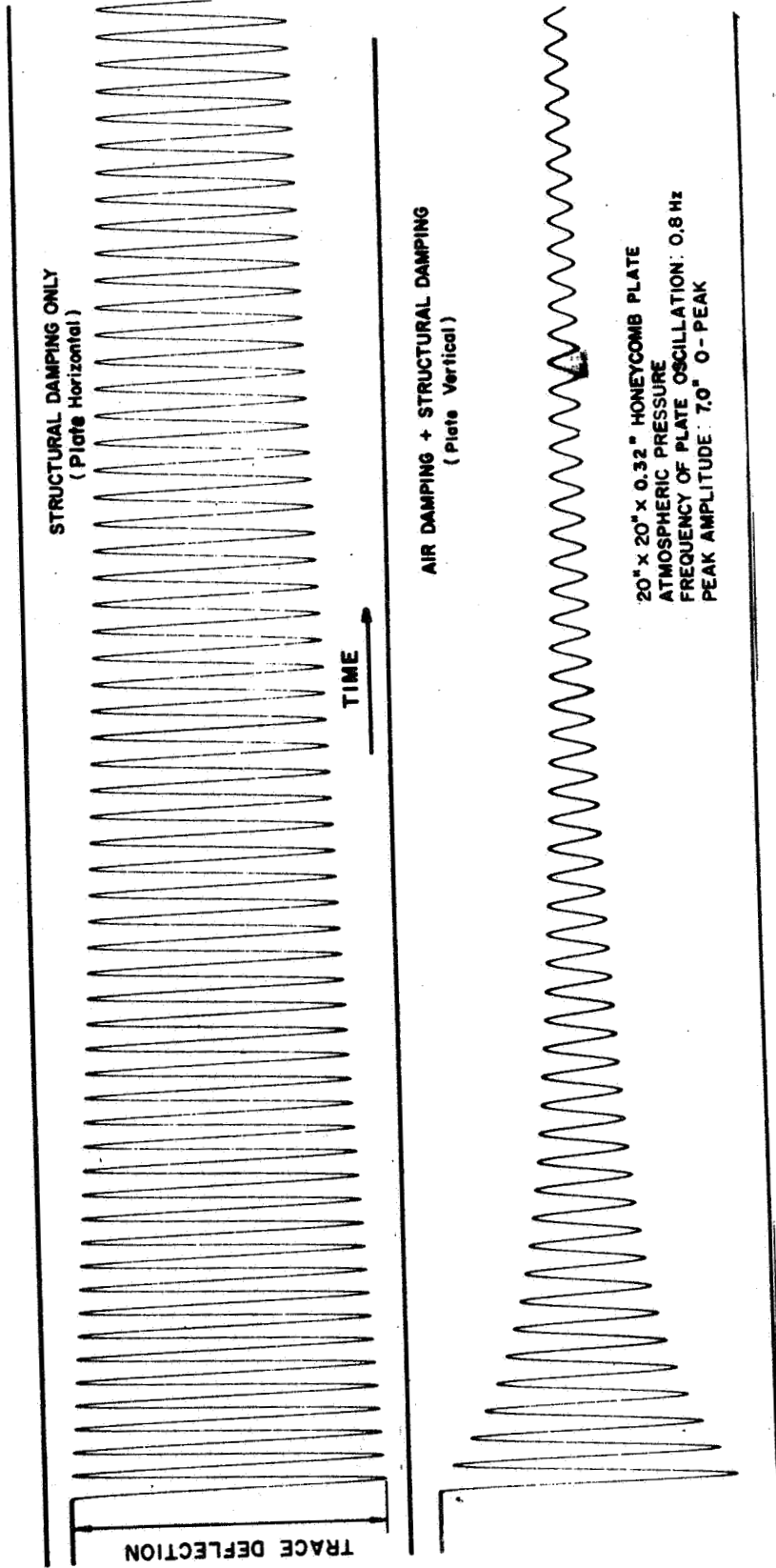


FIGURE 6. FREE DECAY OF A 20 X 20 X 0.16-IN. PLATE

direction normal to its face; in other words, panel pitching is eliminated. The test apparatus was designed to conduct test runs on square plates ranging from 10 × 10 up to 40 × 40 inches.

The only oscillograph data required for the free-decay tests are the decaying amplitudes of oscillation, as a function of time. A Rotary Variable Differential Transformer (RVDT) was used to sense the decaying sinusoid. The RVDT was located at the point of rotation (see Fig. 5) and on the center-line of the flexural springs. The signal from the RVDT was then amplified and recorded on an oscillograph.

An equivalent spring rate (Table 1) for the plate-pendulum system was obtained from the slope of the force versus plate deflection curve.

TABLE 1. - EQUIVALENT MASSES AND SPRING RATES
FOR THE FREE-DECAY TESTS

<u>Plate Size</u>	<u>Equivalent Mass</u>	<u>Equivalent Spring Rate</u>
$b \times b$, in.	$m_e, \frac{\text{lb sec}^2}{\text{in.}}$	$k_e, \frac{\text{lb}}{\text{in.}}$
40 × 40 plain edge	0.0299	0.478
20 × 20 thin edge	0.0312	0.500
20 × 20 plain edge*	0.0336	0.527
10 × 10 thin edge	0.0321	0.513
10 × 10 plain edge	0.0321	0.513
20 × 20 plain edge*	0.0165	0.152
20 × 20 plain edge*	0.0165	0.540

*Used for determination of frequency effects on \tilde{C}_d .

From a plot of the plate deflection versus the deflection of the galvanometer trace on the recording oscillograph, a calibration constant (3.6-in. plate deflection/in. galvanometer deflection) was obtained and used to calculate the amplitude of plate oscillation.

It was important for the purposes of increased accuracy in data reduction that the structural damping of the system be as low as possible. The rates of decay observed with the plate in the horizontal position, i. e., where the air damping is negligible, were an order of magnitude smaller than the expected values for the rates of decay as a result of air damping.

The variables which are required for calculating the oscillatory drag coefficient are shown in the equation:

$$\tilde{C}_d = \frac{3}{4} \frac{\delta_a m_e}{\rho_a x_0 S} \quad (1)$$

The derivation of the above equation is presented in a later section. The following test procedure was used to obtain the values in the equation

$$\delta_a = \delta_a + s - \delta_s$$

To Obtain $\delta_a + s$

- (1) The plate is mounted in a vertical position.
- (2) Forces and deflections in a direction normal to the plate are obtained. From these data and knowing the galvanometer trace recorded on the oscillograph, an equivalent spring constant and an amplitude calibration factor can be obtained (see Table 1).
- (3) The plate is deflected to a maximum initial amplitude, 7 in., zero to peak. The plate is held by a string, the string is burned and the plate oscillations are allowed to decay.
- (4) As the plate oscillations decay, step attenuators on the amplifiers are varied in the following ratios: 1000:700:500:300:200:150:100:70:50. This provides increased accuracy as the plate oscillations become smaller. Data were suitably accurate from 7 in. down to 0.25 inch.
- (5) In order to eliminate unusual discrepancies in the data and also provide sufficient data for numerical curve fitting, five test runs are made with the plate in the vertical position.
- (6) The double amplitudes which are recorded on the paper oscillograph are measured manually for each single cycle of oscillation (see Fig. 6). The logarithmic decrement is calculated using the relationship

$$\delta = \frac{1}{N} \ln \frac{x_i}{x_{i+N}} \quad i = 0, 1, 2, 3, \dots, \text{ etc.}$$

where N is the number of cycles over which the logarithmic decrements are calculated. As the damping decreases at lower amplitudes, then the decrement is calculated for N = 3 and N = 5. After the five runs were completed and the log decrements were plotted versus amplitudes of plate oscillation, a digital technique was used to "best fit" the data to either a straight line or a quadratic function depending on the degree of the polynomial required to match the data.

To Obtain δ_s

- (1) The plate is rotated 90 deg about its horizontal axis, thus providing a minimum drag frontal area.
- (2) The system is allowed to freely oscillate in order to determine any changes of period which might occur as a result of virtual mass of the air. If there is a detectable period change, then low profile lead masses are added until the period for the oscillations in the horizontal mode of operation is identical to that of the vertical mode; i. e., the system is tuned.
- (3) The plate is then deflected to the maximum amplitude, and the decay test procedure outlined previously is repeated.
- (4) The system was extremely low damped, and it was decided to use N = 20, from which the log decrement then becomes

$$\delta_s = \frac{1}{20} \ln \frac{x_0}{x_{20}}$$

- (5) The δ_s is plotted versus the peak amplitude of the decaying sinusoid, and a best fit is obtained for the experimental data in the same manner as for $\delta_a + s$.

To Obtain δ_a

- (1) From the previous two runs, a polynomial equation was fitted to the data such that $\delta = f(x)$, for both δ_a and $\delta_a + s$.
- (2) From these polynomial data fits, the logarithmic decrement as a result of air damping is calculated using the relationship

$$\delta_a = \delta_a + s - \delta_s.$$

Using these data and the relationship $\tilde{C}_d = 3/4 \frac{\delta_a m_e}{\rho_a x_0 S}$, the values of

\tilde{C}_d at various amplitudes can be calculated providing \tilde{C}_d versus $\frac{x_0}{b}$ curves

similar to those in References 4, 5, and 6. The equivalent mass m_e is calculated from the relationship:

$$m_e = \left[\frac{k_e}{(2\pi f_p)^2} \right] = \left[\frac{k_e \tau^2}{(2\pi)^2} \right] \quad (2)$$

The value k_e is the spring rate which was determined from static deflection tests, and τ is the damped period of the complete oscillating system. The values of both k_e and m_e for the different plate sizes are tabulated in Table 1. The equivalent mass is the mass which if located at the center of the plate and supported by a spring of rate k_e would provide a period τ . The value m_e includes the virtual mass of the air, the transfer mass of the pendulum, and the mass of the plate. Estimates of the magnitude of the virtual mass are presented later in the report.

The Forced Vibration Method

The forced vibration test required the accurate measurement of the aerodynamic forces, using a combined dynamometer and an electrical inertia cancellation system. Using this technique, it is possible to cancel out plate inertia. The results obtained from the forced vibration tests appeared to be less accurate than the results from the free-decay tests because of the following:

- (1) The aerodynamic forces on the plate are very small.
- (2) The air inertia effects on the plate, i. e., the virtual mass, cannot be eliminated using the inertia cancellation system.
- (3) The virtual mass forces are of the same order of magnitude as the aerodynamic forces.
- (4) With the plate rotated 90 deg for inertia cancellation there is still a profile drag which cannot be eliminated. As a result, exact inertia cancellation is difficult to obtain.

In the following paragraphs, the forced vibration test apparatus is discussed, and the test procedure is outlined.

Test Apparatus. - The apparatus used for the forced vibration tests is illustrated in Figures 7 and 8. The low frequency vibrator consists of an aluminum table guided on low friction, linear ball bushings. The table is oscillated by an eccentrically mounted crank arm driven sinusoidally by a hydraulic motor. The acceptability of the sinusoidal input to the table was determined by monitoring the acceleration of the table using a strain gage type accelerometer. The reason this restriction was placed on the sinusoidal

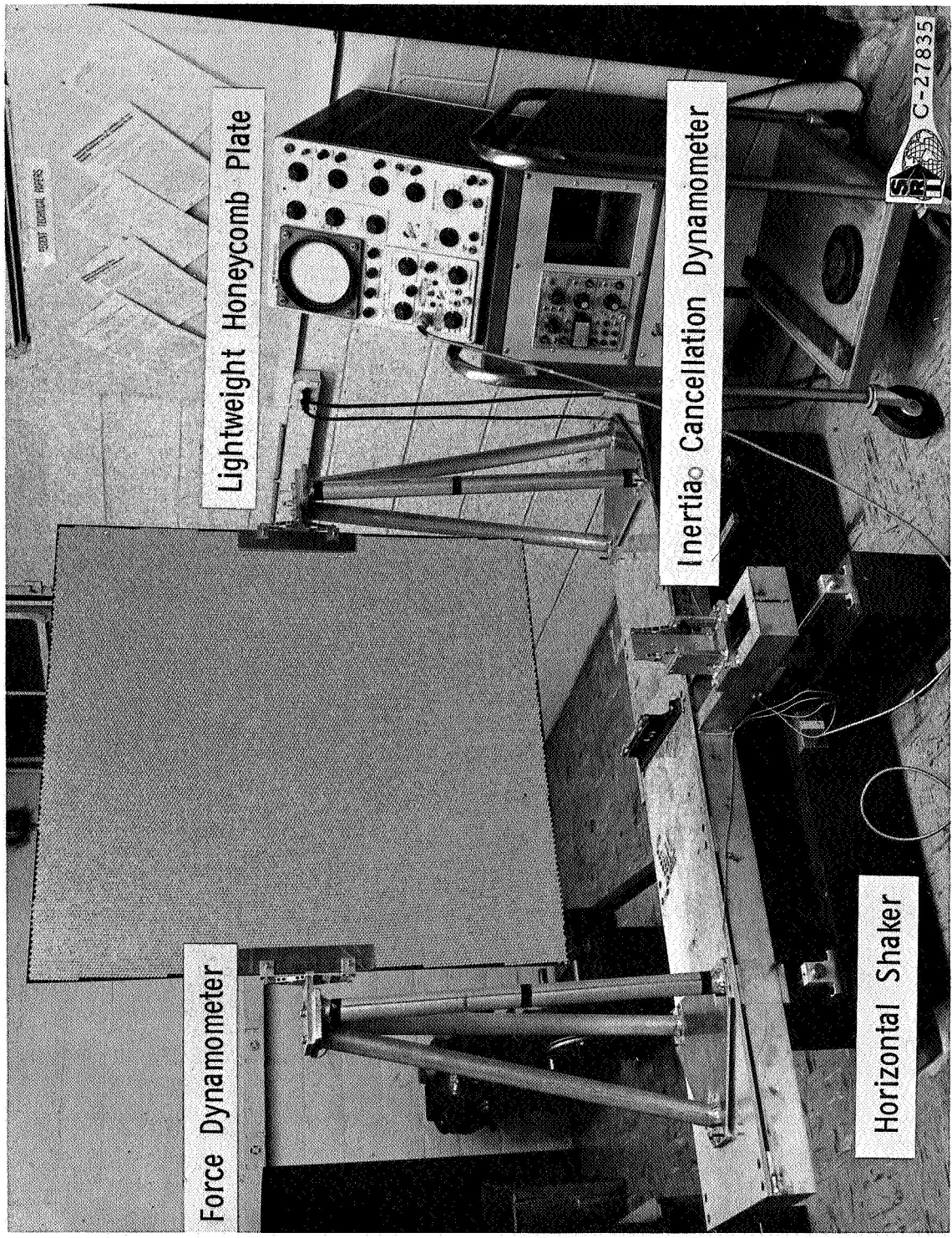


FIGURE 7. LARGE AMPLITUDE HORIZONTAL OSCILLATOR

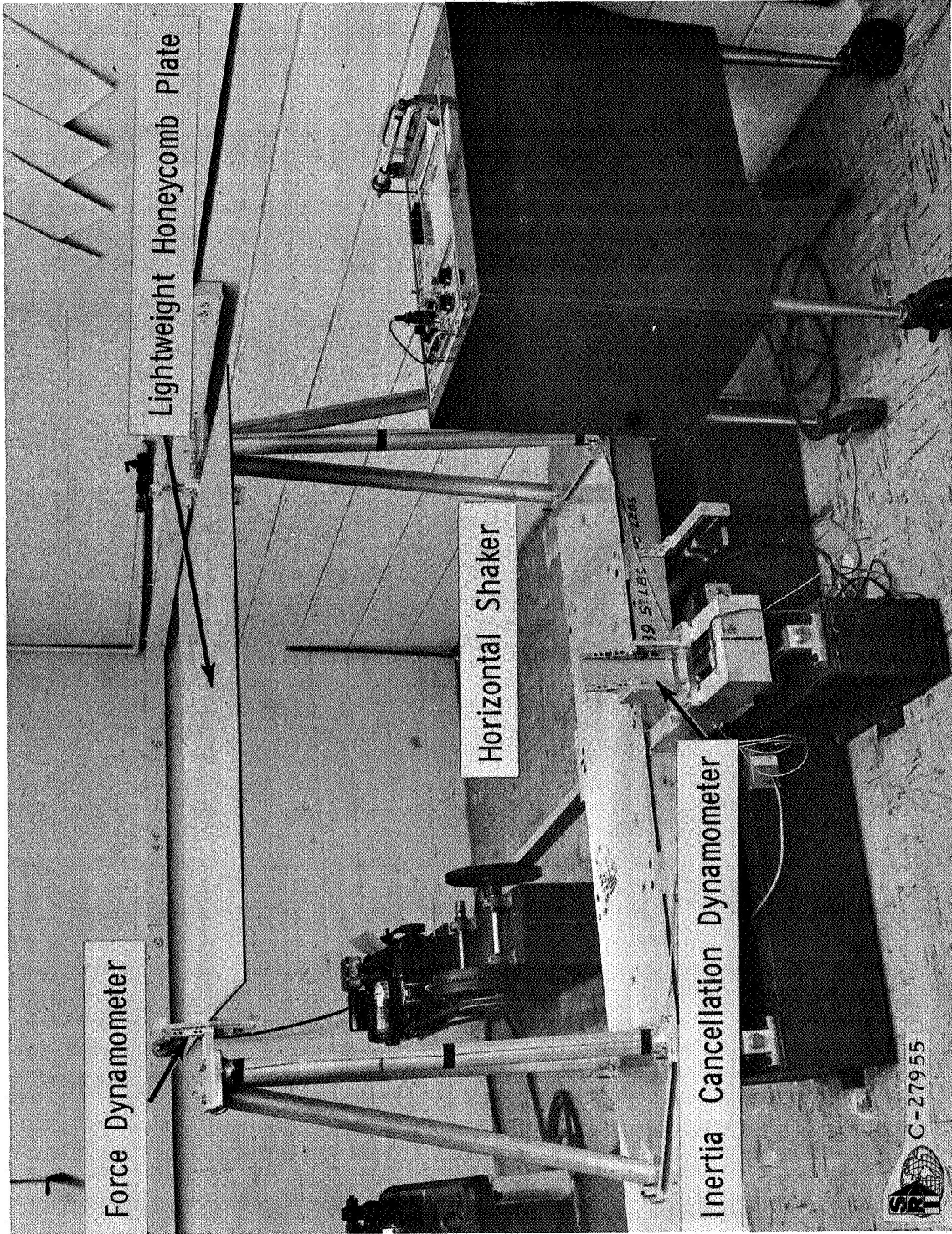


FIGURE 8. PANEL IN HORIZONTAL POSITION FOR INERTIA CANCELLATION

input to the system was because the inertial force components of the plate and the virtual mass which are both to be cancelled are acceleration sensitive, whereas the drag forces are proportional to velocity squared. For this reason, it is beneficial to place a restriction on the acceleration sinusoid even though it is a very stringent restriction. The system was considered acceptable up to a 4-in. single amplitude and from 0.5 to 2.5 Hz.

The plates are mounted on a pair of dynamometers illustrated in Figure 9. A second identical pair of dynamometers mounted on the shaker table (Fig. 10) are wired electronically in a bridge along with the first pair so inertia forces experienced by the plate force dynamometer can be identically cancelled by addition of the proper amount of mass to the inertia cancellation dynamometer. The distance between dynamometers for the 40 × 40-in. plate made the supporting of the plates even more difficult, and it was necessary to use an equivalent mass solid aluminum bar for mass cancellation. A Linear Variable Differential Transformer (LVDT) was used both for measuring the amplitudes of oscillation and for determining the location on the force trace where the velocity was a maximum and acceleration (or inertia components) was zero.

Test Procedure. - The following steps are required to complete a single test run on the forced vibration system:

- (1) The plate is mounted in a horizontal position and locked rigidly in place, as shown in Figure 8.
- (2) With the shaker operating at the test conditions and with the plate horizontal, mass is added to the cancellation dynamometer until a phase change is detected in the force output.
- (3) Since the residual signal does not go exactly to zero, it was decided to obtain a zero force output at the peak acceleration. The reason the residual signal does not reach exact zero throughout the cycle of oscillation is that with the plate in the horizontal position; it still presents a finite profile and the panel still experiences a measurable drag force.
- (4) With the residual signal established, the force measuring dynamometers then must be calibrated. Various masses, amplitudes of oscillation, and frequencies were used to generate a trace deflection versus dynamic force curve with the dynamic force calculated as

$$F = (2\pi f_p)^2 x_o m$$

- (5) The plate is then rotated 90 deg to the vertical position (see Fig. 7) and the test runs are made. Both the aerodynamic forces on the

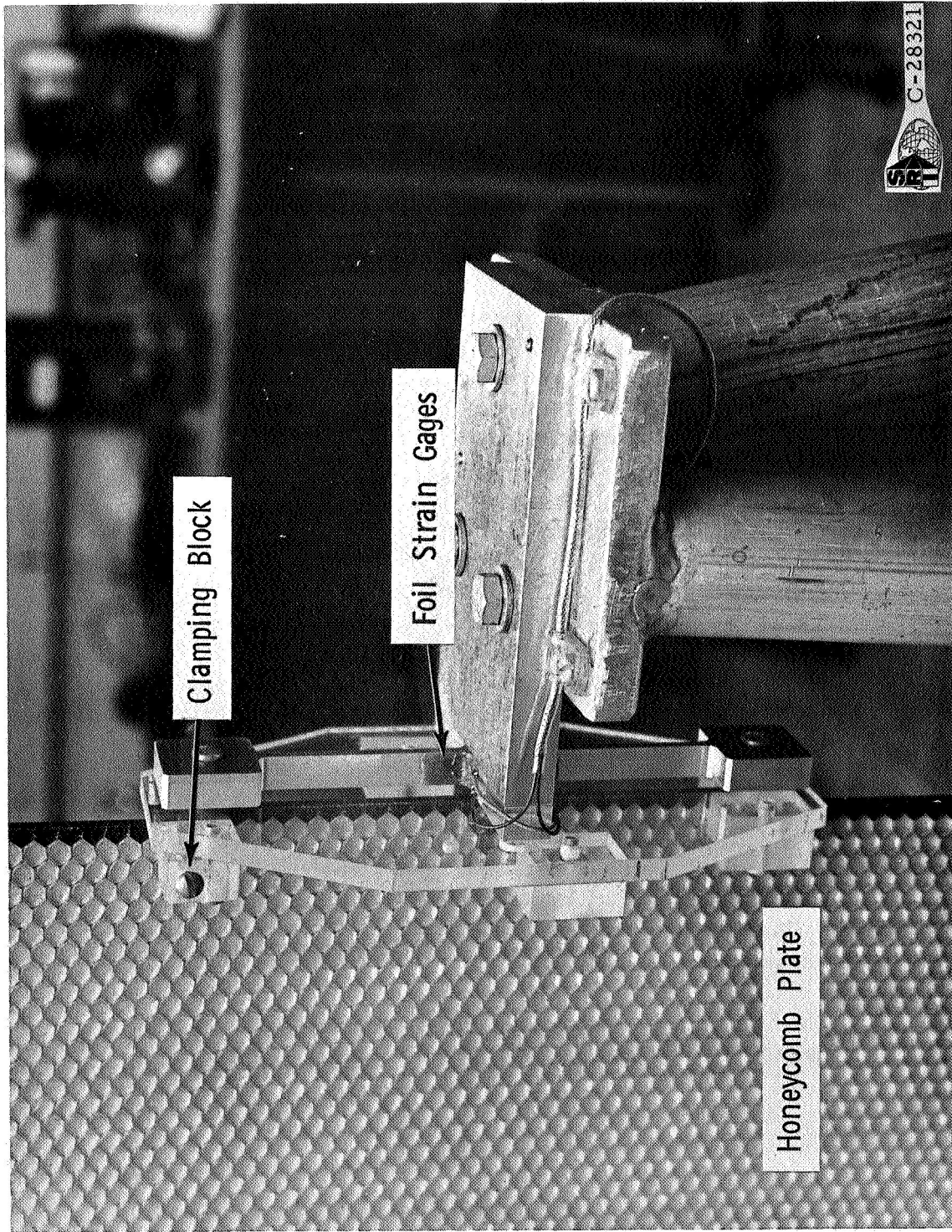


FIGURE 9. DYNAMOMETER USED FOR DRAG FORCE MEASUREMENTS

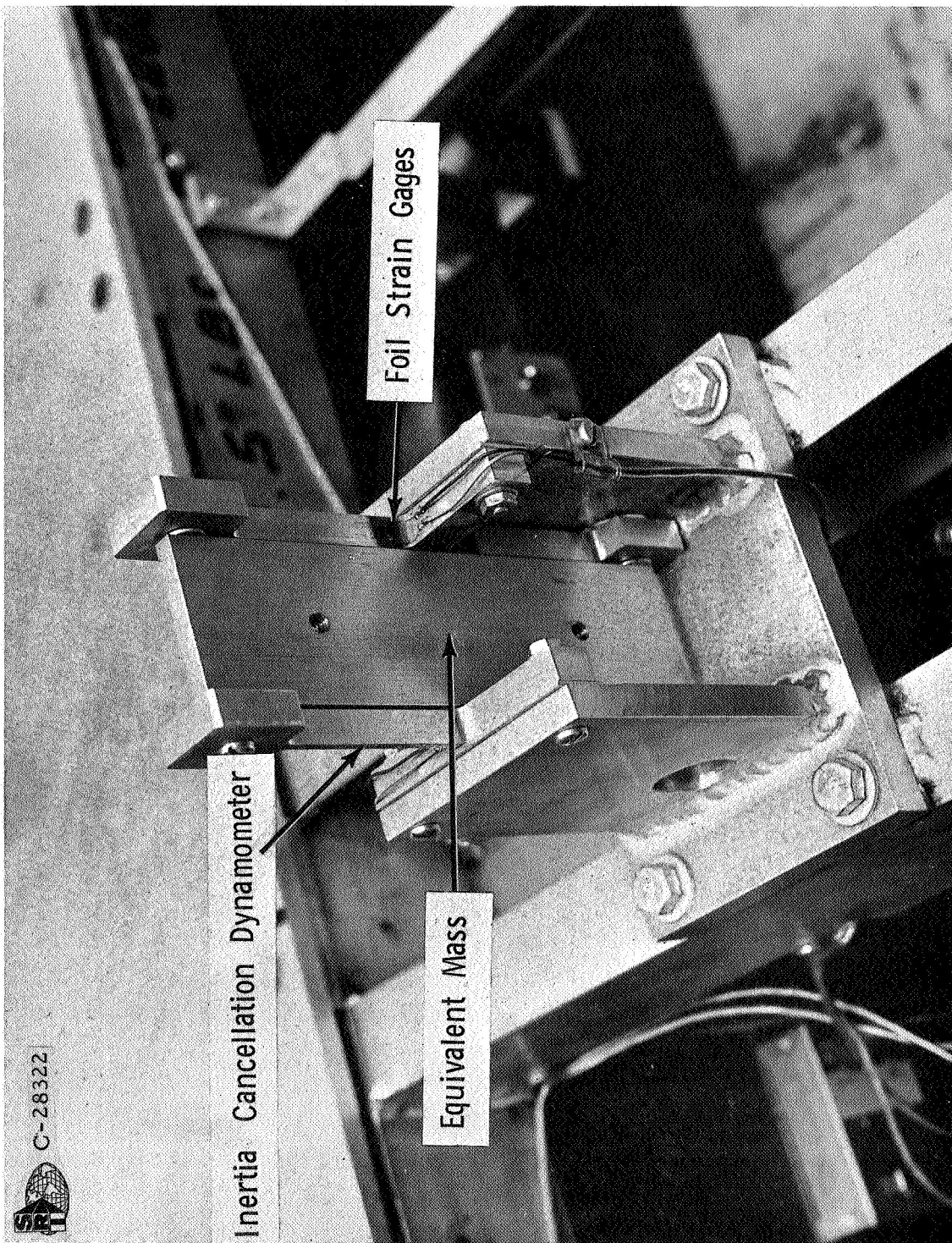


FIGURE 10. DYNAMOMETER USED FOR INERTIA CANCELLATION

plate and the amplitude phase angles are recorded simultaneously on a strip recorder, as shown in Figure 11.

- (6) The drag coefficient is calculated using the force at the point during the cycle where the velocity is a maximum and the inertia terms are zero. The oscillatory drag coefficient is then computed from

$$\tilde{C}_d = \left[\frac{2\tilde{F}_d}{\rho_a(2\pi f_p x_o)^2 S} \right]$$

- (7) The oscillatory drag coefficient is calculated for cases where the amplitudes are varied from 0.5- up to 4.0-in. amplitude, and then values of \tilde{C}_d versus $\frac{x_o}{b}$ can be plotted and compared to the values obtained from the free-decay method.

ANALYSIS

The following paragraphs discuss the analysis which provides the relationships from which the oscillatory drag coefficients are calculated for both the forced and free vibration tests.

Free-Decay Method

The mechanical oscillator and plate are shown in Figure 12 along with the proposed mechanical model of the system. The differential equation for the single degree-of-freedom system with a nonlinear quadratic damping law is

$$m_e \ddot{x} + \frac{1}{2} \rho_a |\dot{x}| \dot{x} \tilde{C}_d S + k_e x = 0 \quad (3)$$

The solution of the nonlinear differential equation is obtained by Minorsky's theory of first-order approximation in Reference 10 as

$$\frac{x_o}{x_1} = \left[1 + \left(\frac{4}{3} \frac{\rho_a x_o \tilde{C}_d S}{m_e} \right) \right] \quad (4)$$

and, by definition of the logarithmic decrement,

$$\frac{x_o}{x_1} = e^{\delta_a} \quad (5)$$

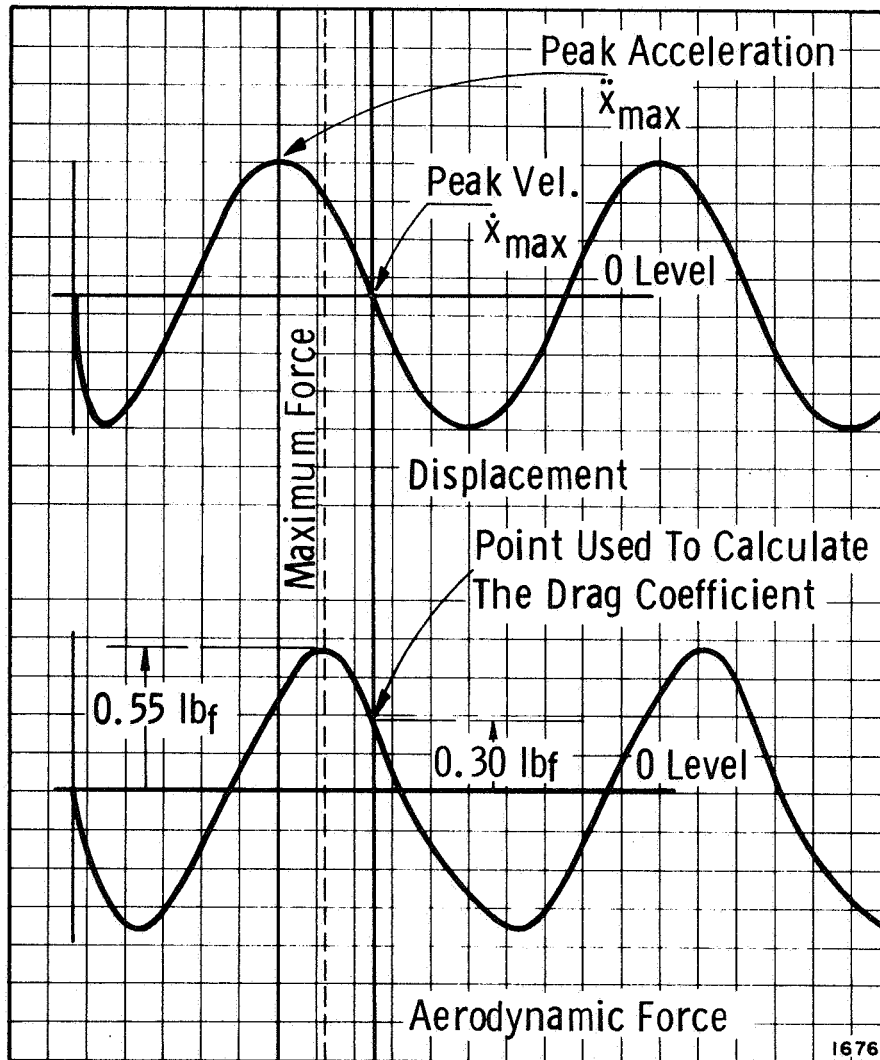
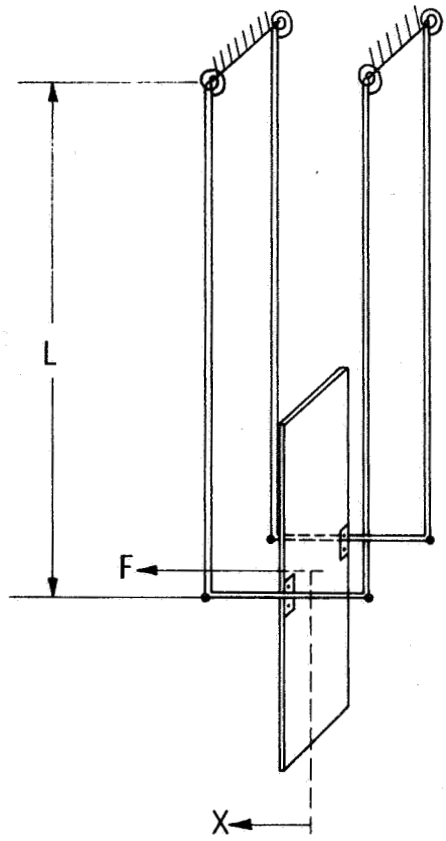
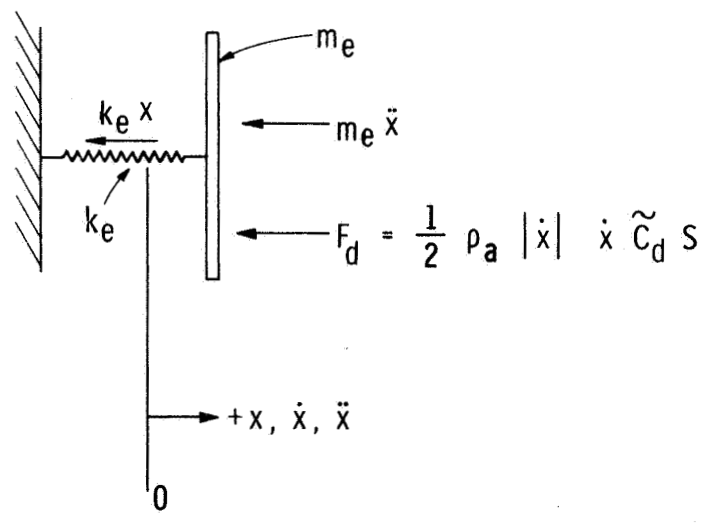


FIGURE 11. DRAG FORCES MEASURED ON A 20 X 20 X 0.32-IN. PLATE OSCILLATED AT AN AMPLITUDE OF 4 IN. 0-Pk AND A FREQUENCY OF 2 Hz



Actual System



Mechanical Model

1285

FIGURE 12. PLATE OSCILLATOR SCHEMATIC

or, by first order of approximation

$$\frac{x_0}{x_1} = 1 + \delta_a \quad (6)$$

and substituting Equation (6) into Equation (4)

$$\tilde{C}_d = \frac{3}{4} \frac{\delta_a m_e}{\rho_a x_0 S} \quad (1)$$

This relationship is used to calculate drag coefficients for the free-decay tests. Some of the conditions which are applied in obtaining this relationship are the following:

- (1) It is assumed that the damping is small, and the amplitude change is small over a single cycle.
- (2) It is assumed that the oscillatory drag coefficient can be considered relatively constant during a single cycle.
- (3) The aerodynamic forces are represented by an equation of the form (see Ref. 7)

$$\tilde{F}_d = \frac{1}{2} \rho_a |\dot{x}| \tilde{C}_d S$$

where the task is placed on obtaining a suitable drag coefficient \tilde{C}_d which might in fact vary with the amplitude of the oscillation.

- (4) It is assumed that the difference in damping going from the vertical plate position to the horizontal plate condition represents the air drag contribution; i. e.,

$$\delta_a = \delta_a + s - \delta_s$$

These four conditions imposed on the analysis are not too unreasonable, and the theory, therefore, should be adequate in predicting the drag coefficients. Not only does it provide a method of computing oscillatory drag coefficients, but it provides a relatively simple method of calculating the successive amplitudes of oscillation from the recurring relationship

$$x_{i+1} = \left(\frac{x_i}{1 + \frac{4}{3} \frac{\rho_a x_i \tilde{C}_d S}{m_e}} \right) \quad (7)$$

Forced Vibration Method

The forced vibration method at first glance appears to be the most straightforward method of obtaining the oscillatory drag coefficients; however, upon closer examination, the problem becomes much more complex. At first, it appears that forced vibration tests can be useful because the peak amplitude is at a constant level as compared to the free-decay method where the peak amplitude is steadily decreasing. It would appear that by measuring the forces over a complete cycle and knowing the varying amplitude simultaneously, we could calculate the varying drag coefficient from the very basic relationship

$$\tilde{C}_d(x, t) = \left\{ \frac{2\tilde{F}_d[x(t)]}{\rho_a [2\pi f_p x(t)]^2 S} \right\} \quad (8)$$

where \tilde{C}_d and \tilde{F}_d are both functions of the instantaneous amplitude $x(t)$.

However, consider the more general case where the total force on the plate is a combination of the aerodynamic drag force and the air inertia or virtual mass type forces; i. e.,

$$F_{\text{total}} = F_{\text{drag}} + F_{\text{inertia}} \quad (9)$$

or

$$F_{\text{total}} = \frac{1}{2} \rho_a |\dot{x}| \dot{x} \tilde{C}_d S + \rho_a b^3 \ddot{x} \tilde{C}_m \quad (10)$$

The form for the inertia component, i. e., $\rho_a b^3 \ddot{x} \tilde{C}_m$, is generally accepted by all investigators of added virtual mass. Values of \tilde{C}_m have been shown by Kuelegan and Carpenter to be from 0.746 to 3.141 (Ref. 4).

Now, if it is assumed that the oscillations of the plate are sinusoidal and of the form

$$x(t) = x_0 \sin(2\pi f_p t) \quad (11)$$

then

$$\dot{x}(t) = 2\pi f_p x_0 \sin\left(2\pi f_p t + \frac{\pi}{2}\right) \quad (12)$$

and

$$\ddot{x}(t) = (2\pi f_p)^2 x_0 \sin(2\pi f_p t + \pi) \quad (13)$$

whereupon

$$F_{\text{total}}(t) = \frac{1}{2} \rho_a (2\pi f_p x_o)^2 \sin\left(2\pi f_p t + \frac{\pi}{2}\right) \left| \sin\left(2\pi f_p t + \frac{\pi}{2}\right) \right| \tilde{C}_d b^2 + \rho_a (2\pi f_p)^2 x_o \sin(2\pi f_p t + \pi) \tilde{C}_m b^3 \quad (14)$$

or, simplifying,

$$F_{\text{total}}(t) = \rho_a (2\pi f_p)^2 x_o b^2 \left[\frac{1}{2} \tilde{C}_d x_o \sin\left(2\pi f_p t + \frac{\pi}{2}\right) \left| \sin\left(2\pi f_p t + \frac{\pi}{2}\right) \right| + \tilde{C}_m b \sin(2\pi f_p t + \pi) \right] \quad (14a)$$

Figure 13 shows the theoretically calculated values for the velocity, drag force, inertia force and total force experienced by an oscillating plate with assumed values of $\tilde{C}_d = 7$ and $\tilde{C}_m = 1.97$. Only at the peak velocity can the drag coefficient \tilde{C}_d be obtained directly (since $\ddot{x} = 0$). This plot also illustrates the fact that for certain conditions the inertia forces are larger than the drag forces, and, in general, they are at least the same order of magnitude. Using the force measured when the acceleration is zero and the velocity is a maximum provides a method for obtaining a value of \tilde{C}_d for a specific amplitude of vibration.

In general, the forced vibration test will provide the following information:

- (1) The instantaneous drag coefficient for a particular amplitude of oscillation can be obtained.
- (2) The relative magnitude of air inertial forces compared to the air drag forces.

Some of the drawbacks associated with the forced vibration tests were the following:

- (1) Measurements of the low amplitude force levels were difficult.
- (2) It was difficult to obtain an acceptable null force level because of a 2.5-Hz pitching mode of the plate/dynamometer combination.
- (3) The force dynamometer and plate supports interfered with the airflow around the plate.
- (4) With the plate in the horizontal position, there was still some drag damping which could not be eliminated.

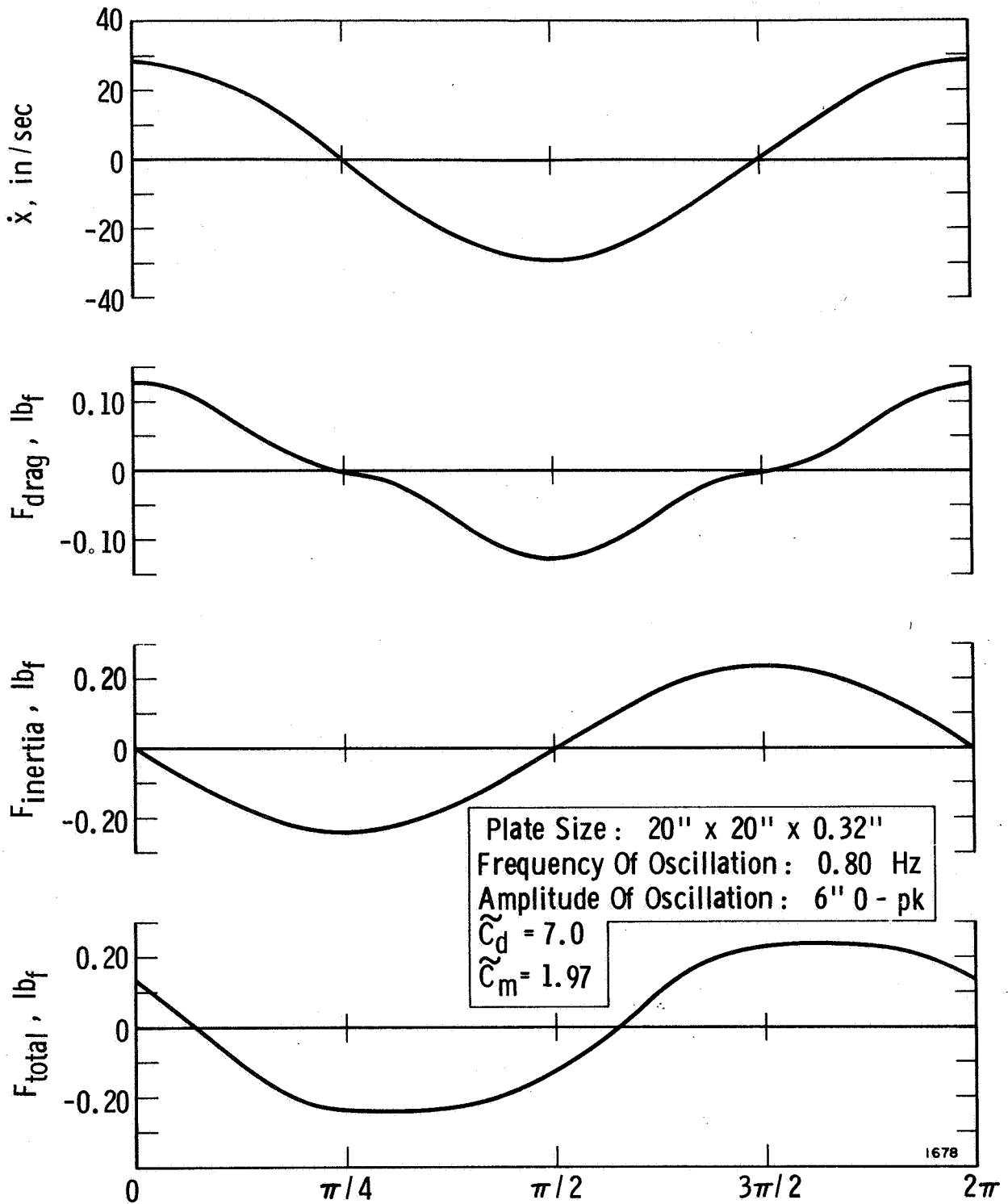


FIGURE 13. THEORETICALLY CALCULATED DRAG, INERTIAL, AND TOTAL FORCES FOR A 20 X 20 X 0.32-IN. PLATE

In the final analysis, the drag coefficients were computed using a steady flow drag equation with a variable drag coefficient; i. e.,

$$\tilde{F}_d = \frac{1}{2} \rho_a (2\pi f_p x_o)^2 \tilde{C}_d S \quad (15)$$

or

$$\tilde{C}_d = \frac{2\tilde{F}_d}{\rho_a (2\pi f_p x_o)^2 S} \quad (16)$$

at the point where the acceleration of the plate is zero, and the velocity is a maximum (see Fig. 11). By conducting tests at amplitudes ranging from $x_o = 4$ in. down to $x_o = 0.5$ in., it is possible to generate a \tilde{C}_d versus $\frac{x_o}{b}$ curve over a limited range. The forced vibration tests extend up to $\frac{x_o}{b} = 0.20$, while the free-decay tests go as far as $\frac{x_o}{b} = 0.60$ for the smaller plates. There is a large amount of scatter in the forced vibration results, particularly at the lower amplitudes where force levels were of the same order of magnitude as the mechanical noise. Even though the results showed scatter in the data, the results for a given condition were repeatable.

In general, the free-decay tests are adequate for taking data which will provide an average oscillatory drag coefficient. The forced vibration tests are useful for observing the inertia forces and the aerodynamic drag forces simultaneously, for obtaining drag coefficients for a constant peak amplitude, and for flow visualization, e. g., by smoke studies. Oscillatory drag coefficients obtained from both test setups are discussed in the following section.

DISCUSSION OF THE RESULTS

The effects of the various parameters on the oscillatory drag coefficients will be presented in the same order they were initially outlined in the "state-of-the-art" discussion. Included in the discussion are the results of virtual mass measurements which were obtained during the studies.

Amplitude

Figures 14 through 17 illustrate the effect of the amplitude variation on the oscillatory drag coefficient. Below each drag coefficient curve are the data from which the oscillatory drag coefficients were calculated. It is observed from these curves that data scatter in the logarithmic decrements at the lower amplitudes can result in large variations in the resulting

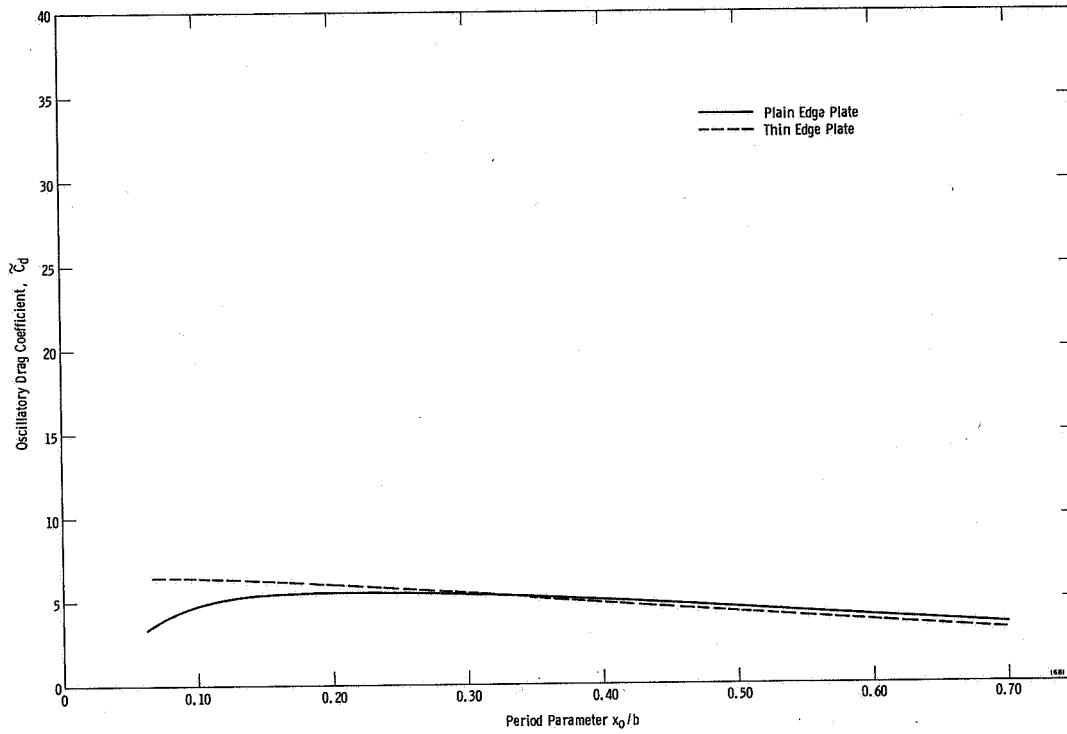


FIGURE 14a. DRAG COEFFICIENT FOR THE 10 × 10 × 16-IN. PLATE AT AN OSCILLATORY FREQUENCY OF 0.63 Hz

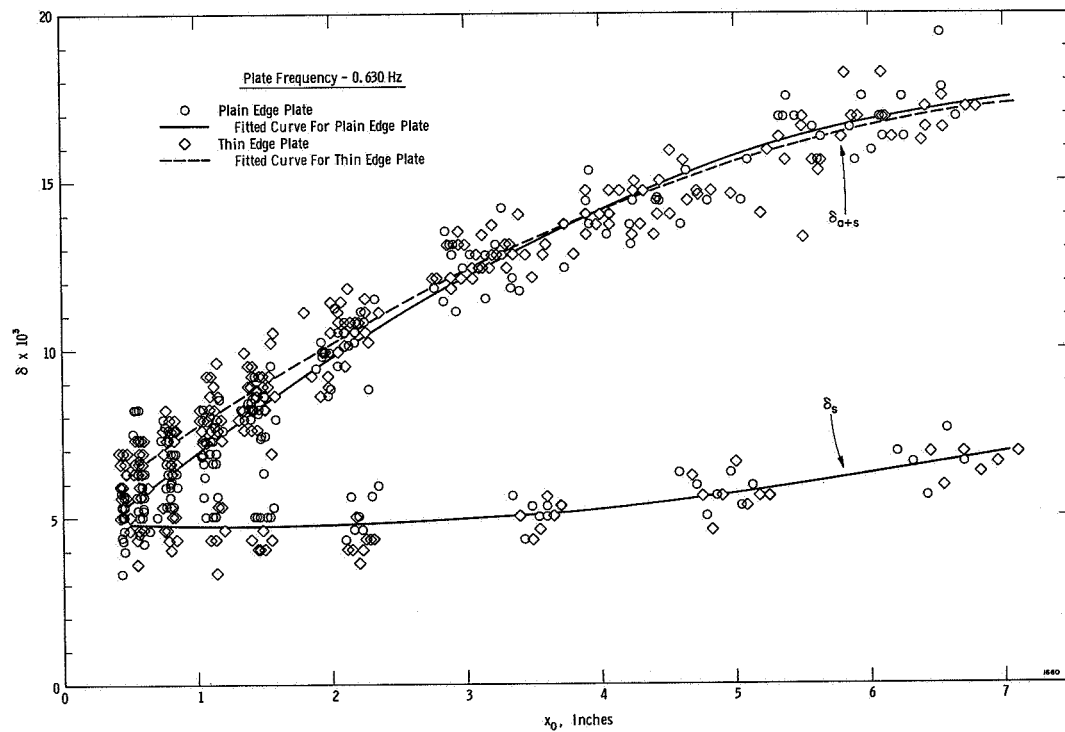


FIGURE 14b. AIR DAMPING FOR A 10 × 10 × 0.16-IN. PLATE OBTAINED BY THE FREE-DECAY METHOD

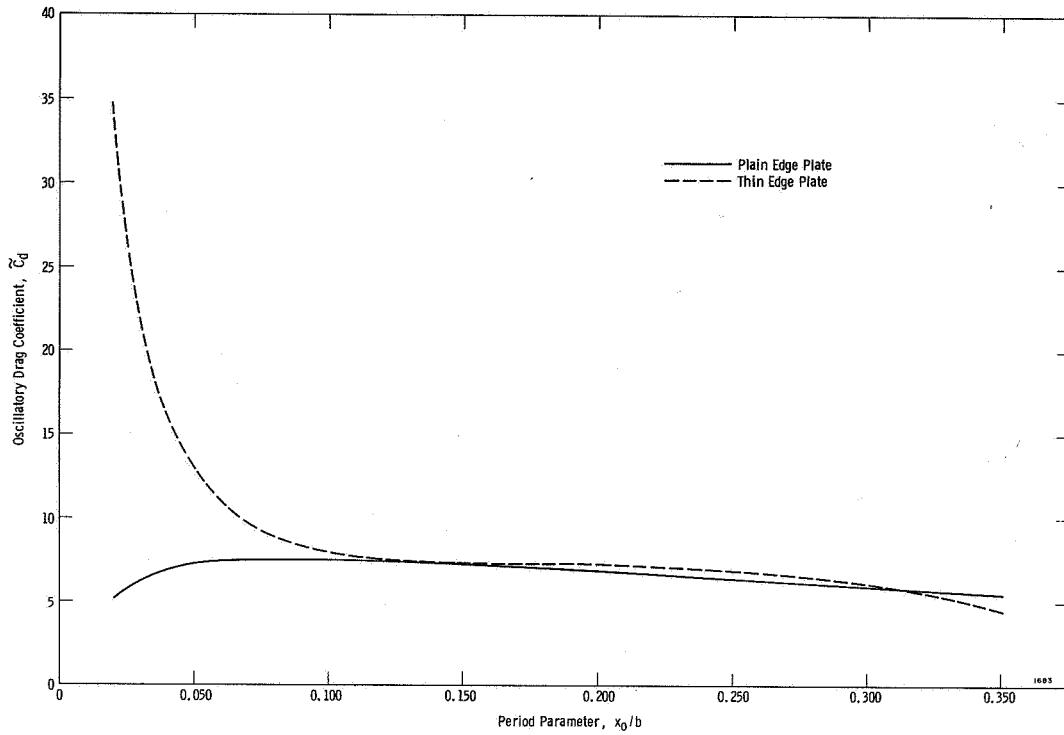


FIGURE 15a. DRAG COEFFICIENT FOR THE $20 \times 20 \times 0.32$ -IN. PLATE AT AN OSCILLATORY FREQUENCY OF 0.63 Hz

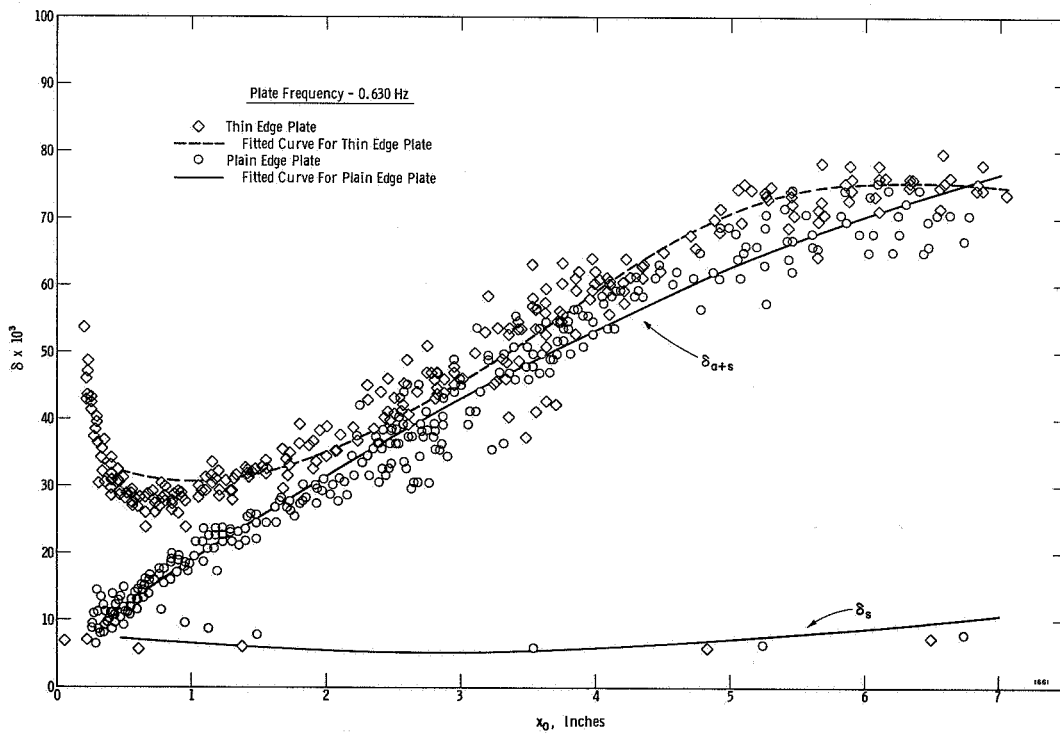


FIGURE 15b. AIR DAMPING FOR A $20 \times 20 \times 0.32$ -IN. PLATE OBTAINED BY THE FREE-DECAY METHOD

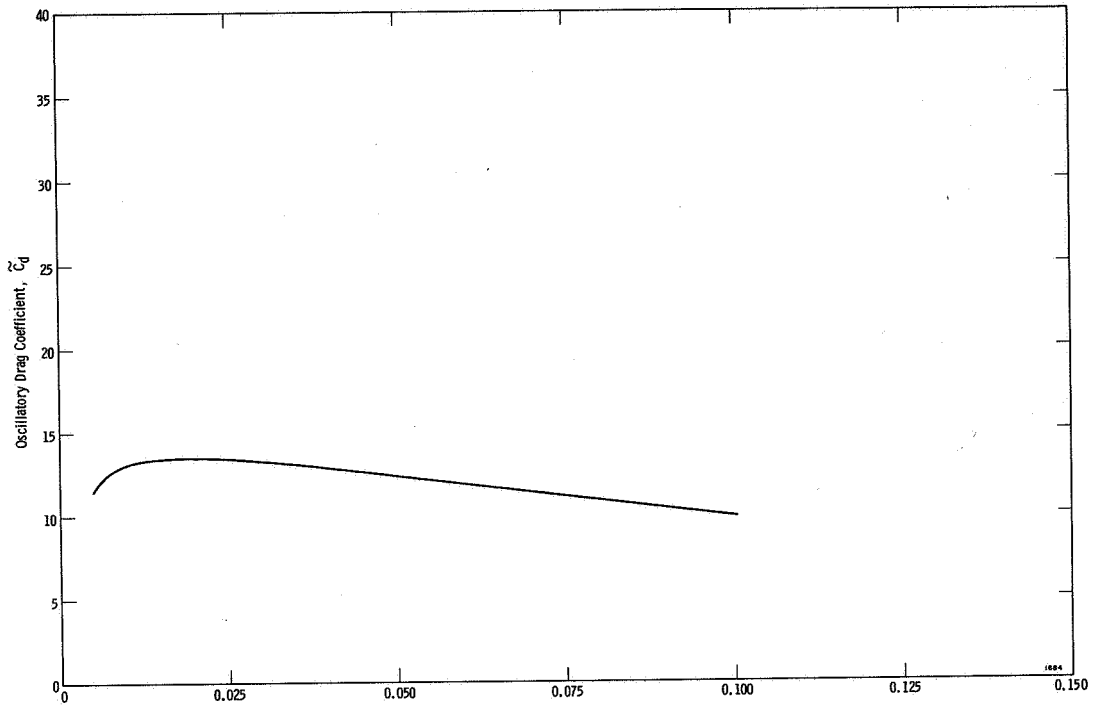


FIGURE 16a. DRAG COEFFICIENT FOR THE 40 X 40 X 0.64-IN. PLATE AT AN OSCILLATORY FREQUENCY OF 0.63 Hz

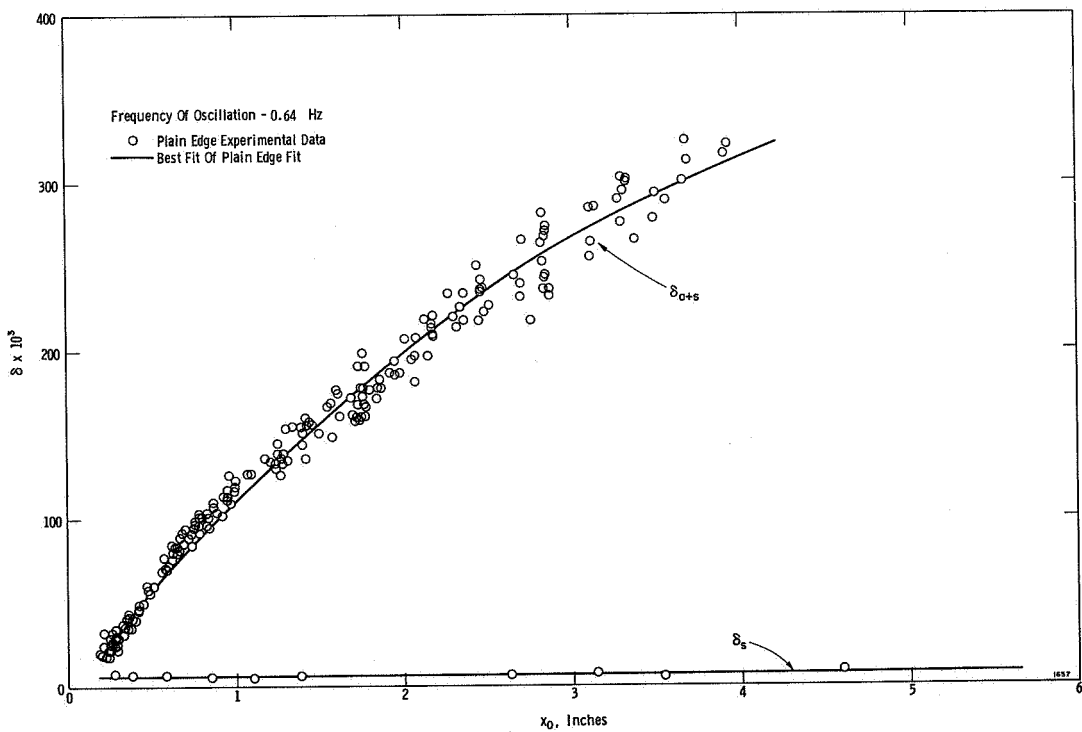


FIGURE 16b. AIR DAMPING FOR A 40 X 40 X 0.64-IN. PLATE OBTAINED BY THE FREE-DECAY METHOD

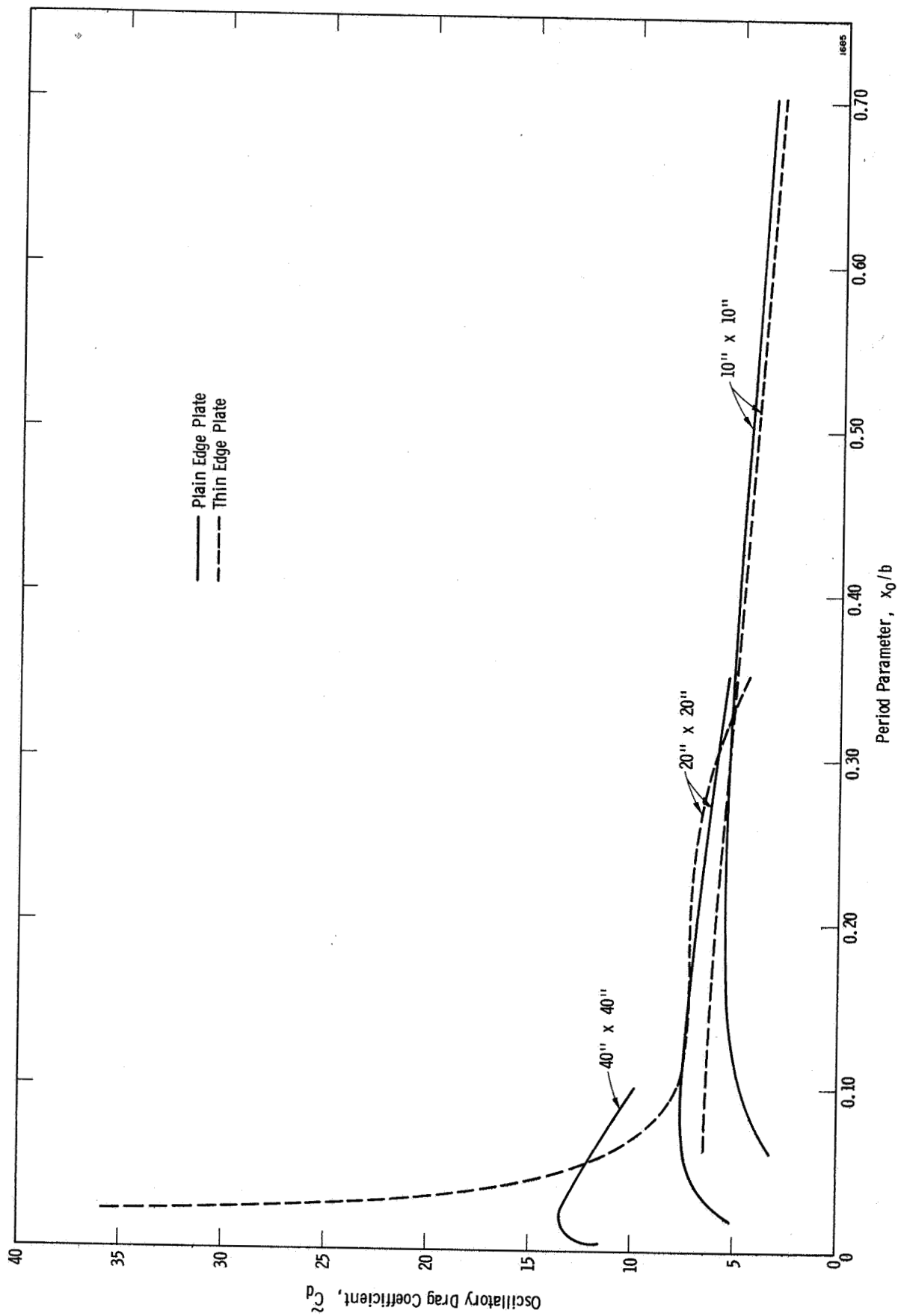


FIGURE 17. SUMMARY OF OSCILLATORY DRAG COEFFICIENT FOR FIVE DIFFERENT PLATES AT 0.63 Hz

oscillatory drag coefficients for the lower ranges of the period parameter. For this reason, it is dangerous to identify definite trends in the range of the smaller period parameters. In general, for a given plate, the oscillatory drag coefficient is constant with the period parameter. It is important to note that the data obtained in the present report were in a very narrow band of the region considered in References 4-6. The fact these data are in a narrow band might explain why the drag coefficients appear constant because a very small period parameter band has been highly amplified.

Frequency

Figure 18 illustrates results of tests which were conducted in order to determine if the drag coefficient was frequency dependent. The frequency variation was from a low frequency of 0.48 Hz up to 0.93 Hz for the highest frequency. For the frequency variation obtained, there was an insignificant variation of the drag coefficient. Figures 19 and 20 illustrate results obtained from forced vibration tests. Using the constant peak amplitude shaker, it was possible to obtain frequencies varying from 0.50 to 2.0 Hz; however, the inaccuracy of the force measurements prevents a definite correlation between the drag coefficient and the frequency parameter.

Thickness

Figure 17 summarizes all the data obtained from both the plain edge and thin edge plates. The thin edge for the 20 × 20-in. plate was 0.012 in., while the thin edge for the 10 × 10-in. plate was 0.007 in. thick. The apparent plate width-to-thickness ratios were 1670 for the 20 × 20-in. plate and 1430 for the 10 × 10-in. plate. In both cases, the thin edge plates are two orders of magnitude thinner than the plain edge plates.

For the larger range of period parameters, there appears no detectable difference between the drag coefficients for the plain and thin edge plates. In the range of smaller period parameters, the thin edge plates appear, in general, to have higher drag coefficients; however, these differences are in a range where the data are less reliable.

Area

Stephens and Scavullo (Ref. 2) in their investigations of air damping recognized that for velocity squared damping the logarithmic decrement obtained from free-decay tests were related to the air density, amplitude, plate mass and plate area in the following manner:

$$\delta_a = 22 \frac{\rho_a x_0 S^{4/3}}{m_e} \quad (17)$$

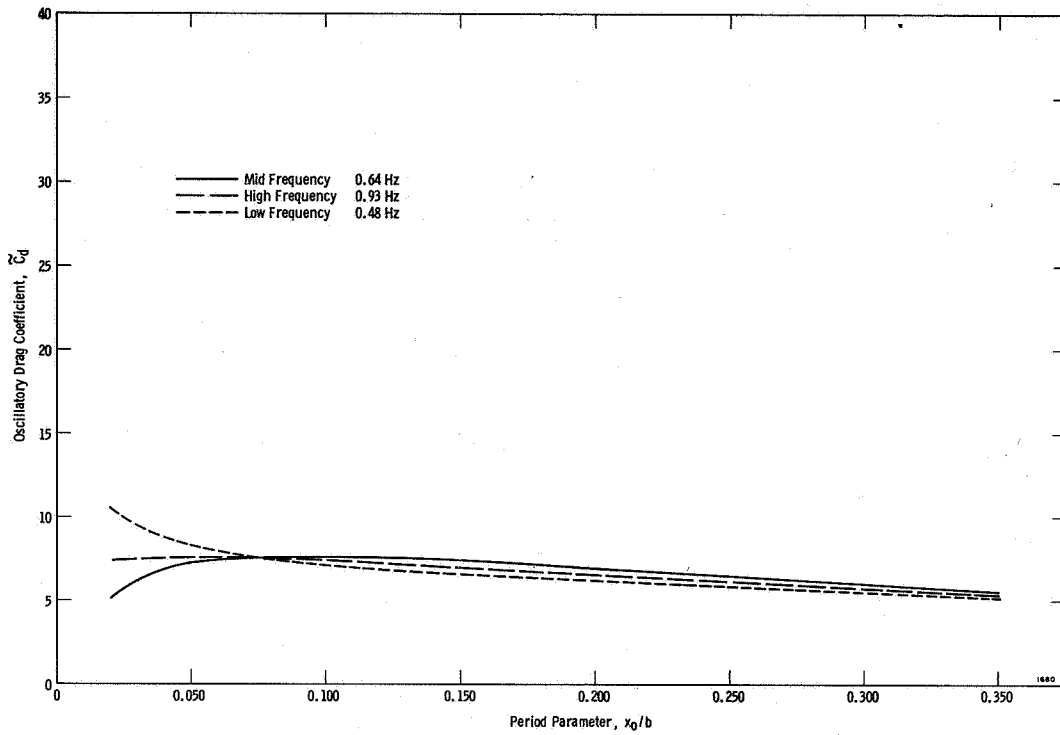


FIGURE 18a. AIR DAMPING OF A $20 \times 20 \times 0.32$ -IN. PLATE WITH A FREQUENCY VARIATION

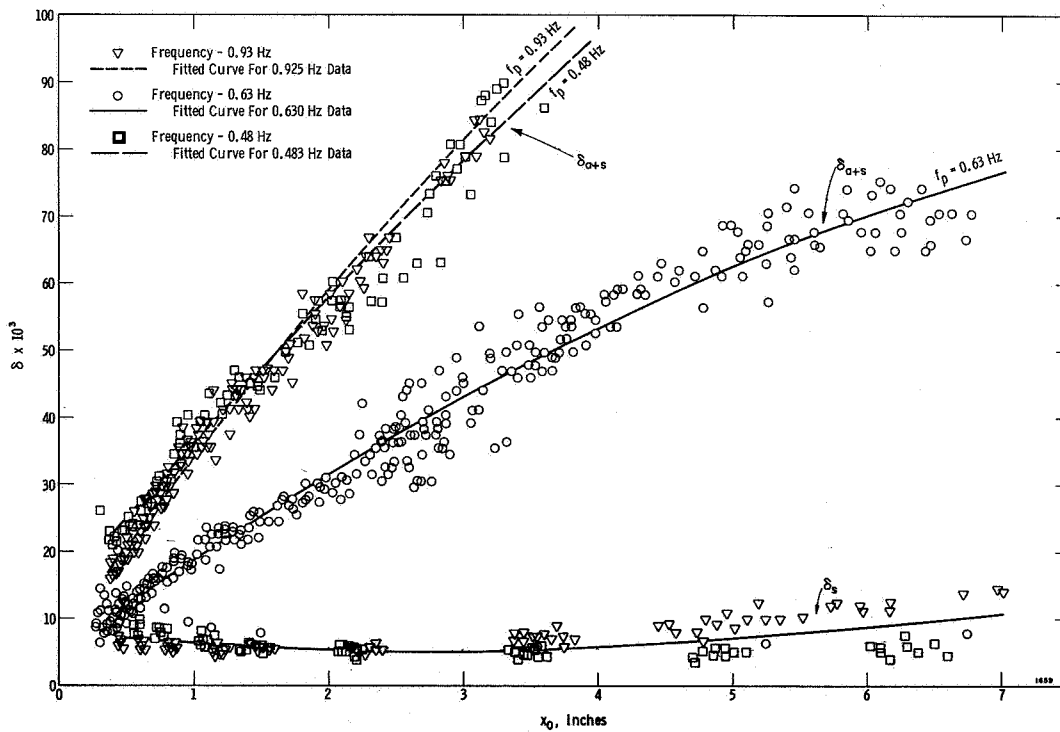


FIGURE 18b. DAMPING OF A $20 \times 20 \times 0.32$ -IN. PLATE OBTAINED BY FREE-DECAY METHOD

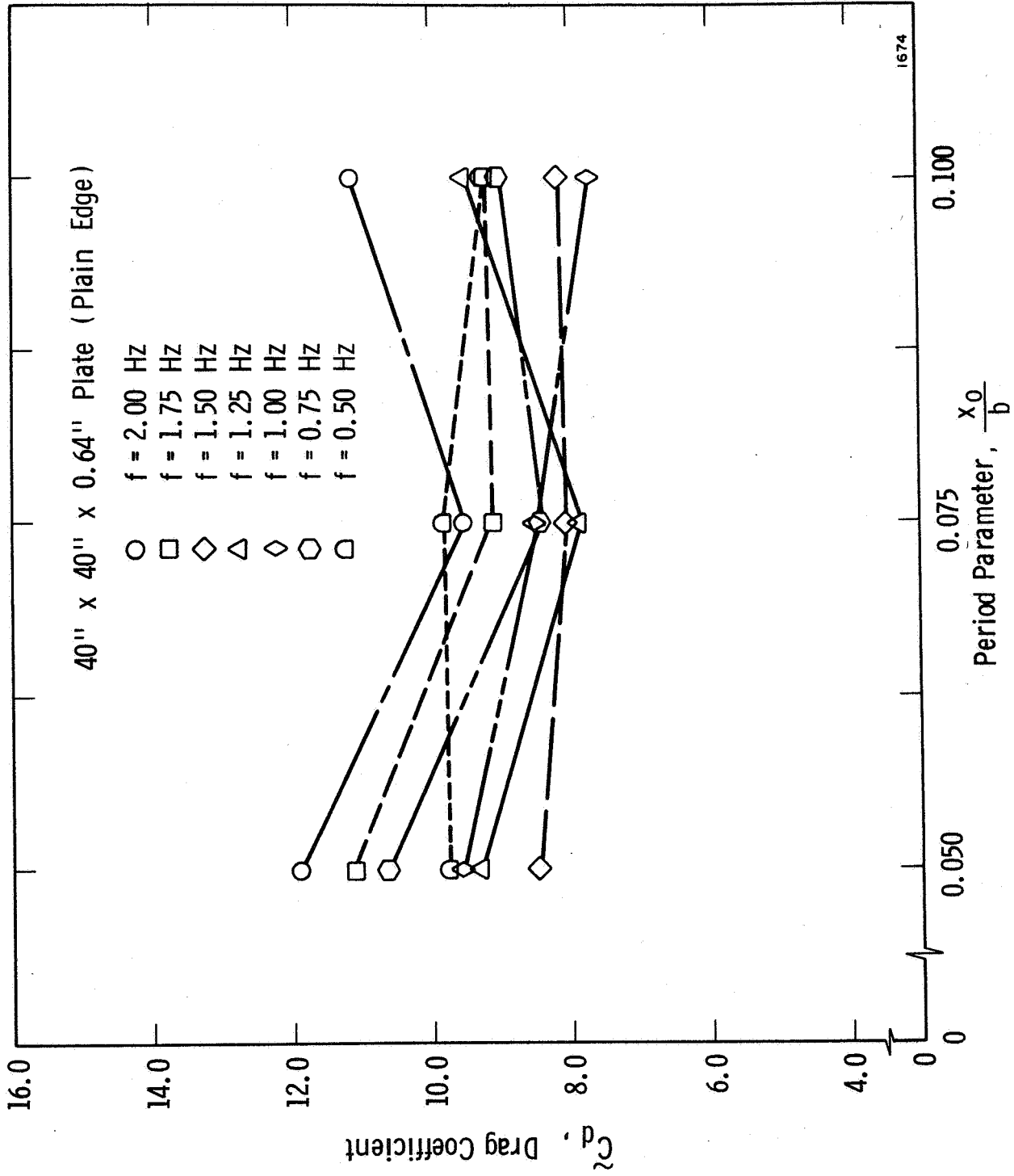


FIGURE 19. DRAG COEFFICIENTS AT VARYING PERIOD PARAMETERS AND FREQUENCIES OBTAINED BY FORCED VIBRATION METHOD

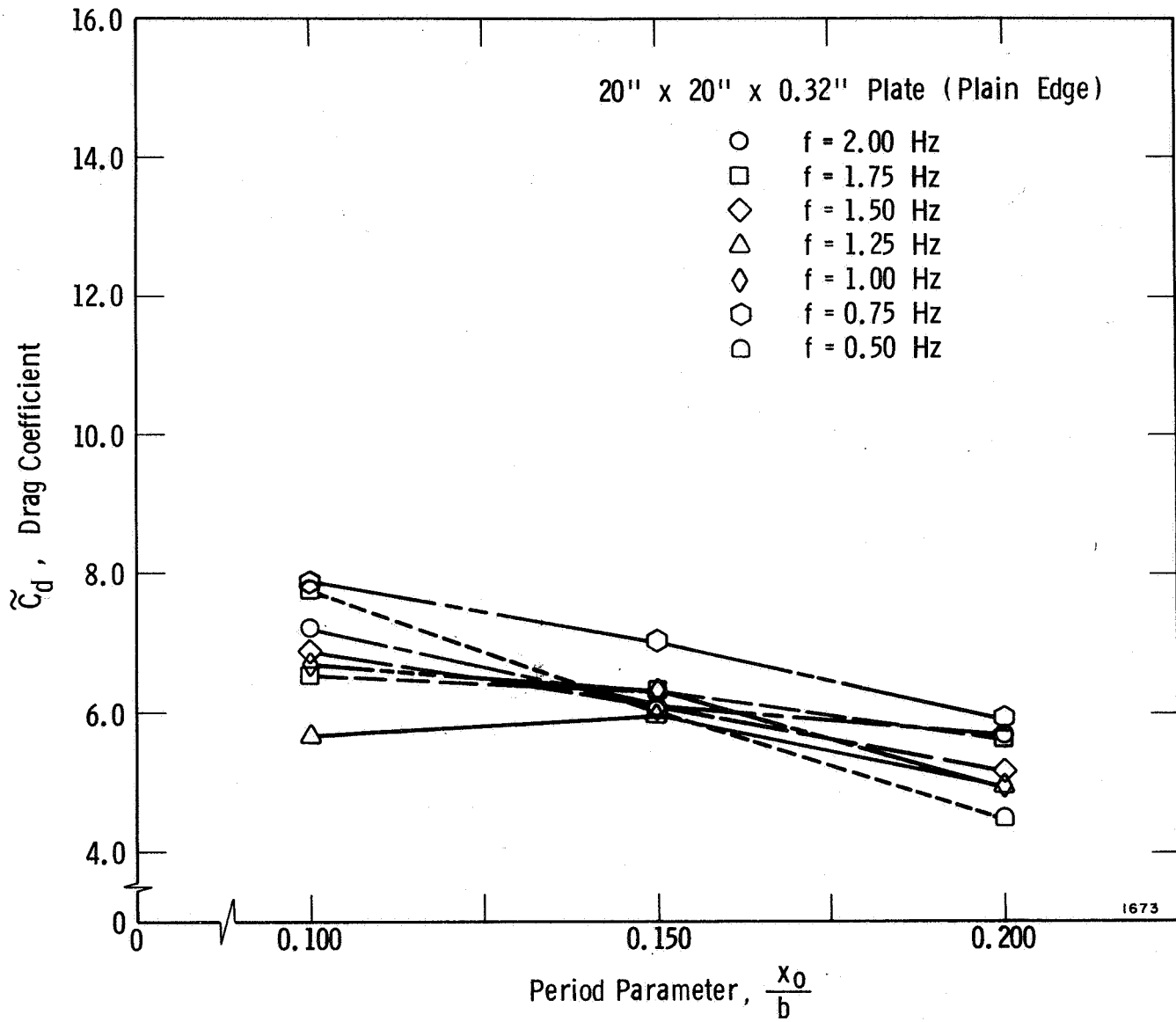


FIGURE 20. DRAG COEFFICIENTS AT VARYING PERIOD PARAMETERS AND FREQUENCIES OBTAINED BY FORCED VIBRATION METHOD

and, earlier in the present report, it was shown that

$$\tilde{C}_d = \frac{3}{4} \frac{\delta_a m_e}{\rho_a x_o S} \quad (1)$$

Substituting Equation (17) into Equation (1) shows that according to Stephens and Scavullo, the oscillatory drag coefficient is

$$\tilde{C}_d = 16S^{1/3} \quad 0.02 \leq \frac{x_o}{b} \leq 0.06 \quad (18)$$

providing S is expressed in sq ft. The results of Stephens and Scavullo (Ref. 2) and also those obtained from the present study are illustrated in Figure 21. The empirical relationship obtained from the present investigation indicates that the drag coefficient varies as

$$\tilde{C}_d = 5S^{1/3} \quad 0.005 \leq \frac{x_o}{b} \leq 0.70 \quad (19)$$

The frequency of oscillation for Stephen and Scavullo's investigation was 3.8 Hz, whereas the present "area effect" investigations were conducted at 0.630 Hz.

In general, the drag coefficient appears to be not only a function of the area but a function of another parameter which has not yet been established.

Virtual Mass

It has been demonstrated earlier in this report that the air inertia forces could easily be of the same order of magnitude as the aerodynamic drag forces. The main difference is that the inertia term primarily affects the natural frequency of the system, whereas the air drag term affects the damping in the system or the decay rate of the oscillations. In order to determine the virtual mass, a separate set of tests was conducted. The virtual mass was calculated by the relationship

$$m_v = \left[\left(\frac{\tau_v}{\tau_h} \right)^2 - 1 \right] m_s \quad (20)$$

where

$$m_s = \frac{k_e}{(2\pi f_p)^2} = \left[\frac{k_e(\tau_h)^2}{(2\pi)^2} \right] \quad (21)$$

based on experimentally obtained values of k_e and τ_h . The total equivalent mass, then, is the sum of the structural mass of the pendulum/plate system,

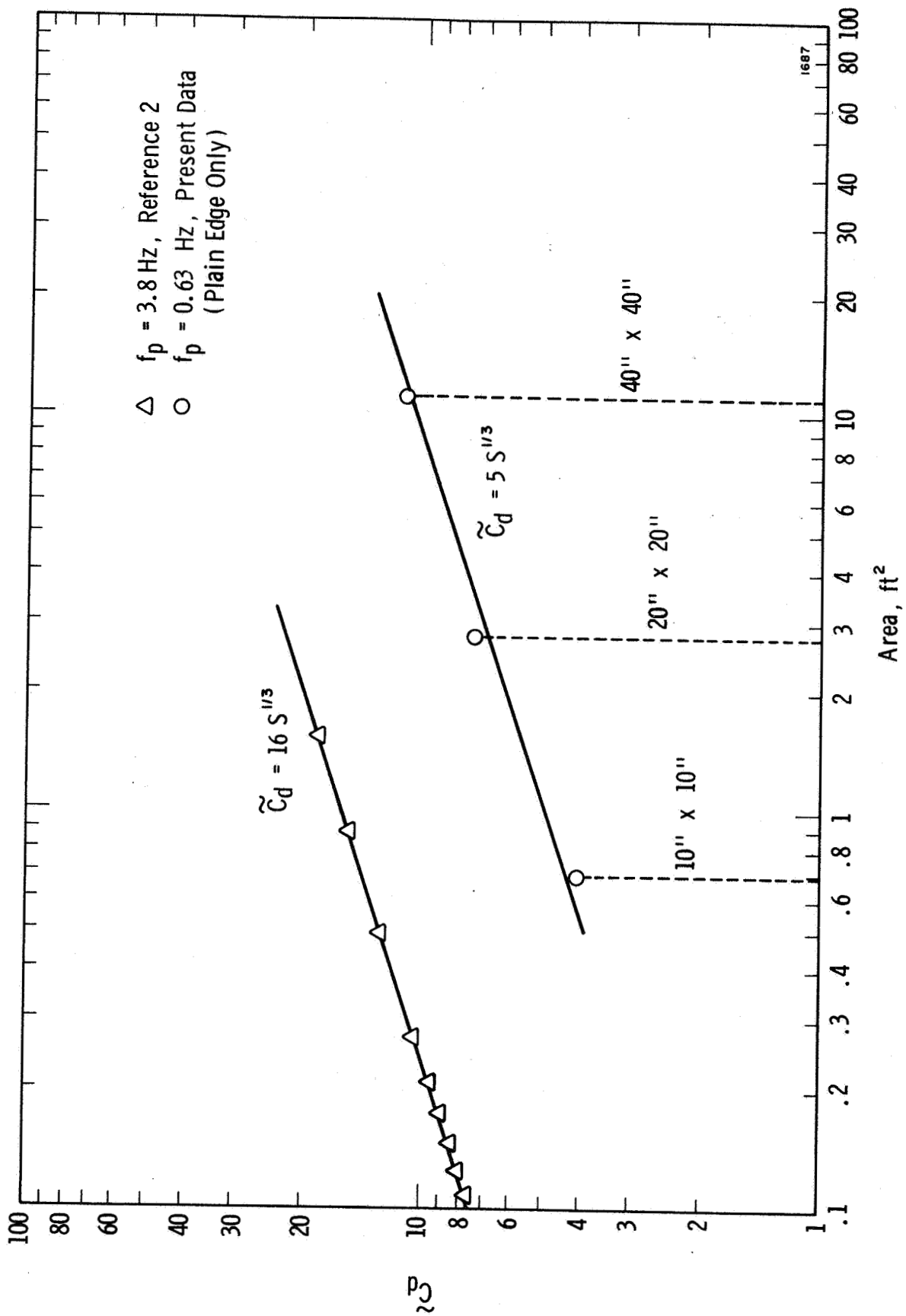


FIGURE 21. VARIATION OF THE DRAG COEFFICIENT AS A FUNCTION OF PLATE AREA

m_s , and the virtual mass of the air, m_v , or, that is,

$$m_e = m_s + m_v \quad (22)$$

The plate is rotated to the horizontal position which will provide the period, τ_h , used in Equation (21) for calculating the structural mass of the system. The value of

$$m_e = \frac{k_e(\tau_v)^2}{(2\pi)^2} \quad (23)$$

shown early in the report from which the oscillatory drag coefficients were calculated contained both the structural mass of the system and the virtual mass of the air.

Figure 22 illustrates the results obtained with the data presented in the form of the virtual mass, m_v , versus the dimension b^3 or

$$m_v = \rho_a b^3 \tilde{C}_m \quad (24)$$

The mass coefficients, \tilde{C}_m , observed by Kuelegan and Carpenter (Ref. 4), for an infinite aspect ratio plate were in the range of $\tilde{C}_m = 0.746$ to 3.141 depending upon the period parameter. The mass coefficients obtained from the present set of tests indicate a value of \tilde{C}_m equal to 0.68 for an aspect ratio of 1.0 and a period parameter of approximately 0.2. Kuelegan and Carpenter did not go to a period parameter less than $\frac{x_0}{b} = 0.27$, at which point they experienced a \tilde{C}_m of 1.35, and the trend of \tilde{C}_m was becoming smaller with smaller period parameters.

ENGINEERING APPLICATION OF OSCILLATORY DRAG COEFFICIENTS

An engineering application which might utilize the data obtained in this report is the case of a large surface area, lightweight, flexible plate which is vibrating as a simple thin cantilever beam. The equation of motion for the free vibration per unit length of a thin, flexible, cantilever beam can be written as

$$\frac{\partial^2 M}{\partial x^2} + \frac{1}{2} b \rho_a \left| \frac{\partial y}{\partial t} \right| \frac{\partial y}{\partial t} + \rho A \frac{\partial^2 y}{\partial t^2} = 0 \quad (25)$$

and for free vibration in the n -th mode with small damping

$$y(x, t) \approx A_n \Phi_n(x) \sin \omega_n t \quad (26)$$

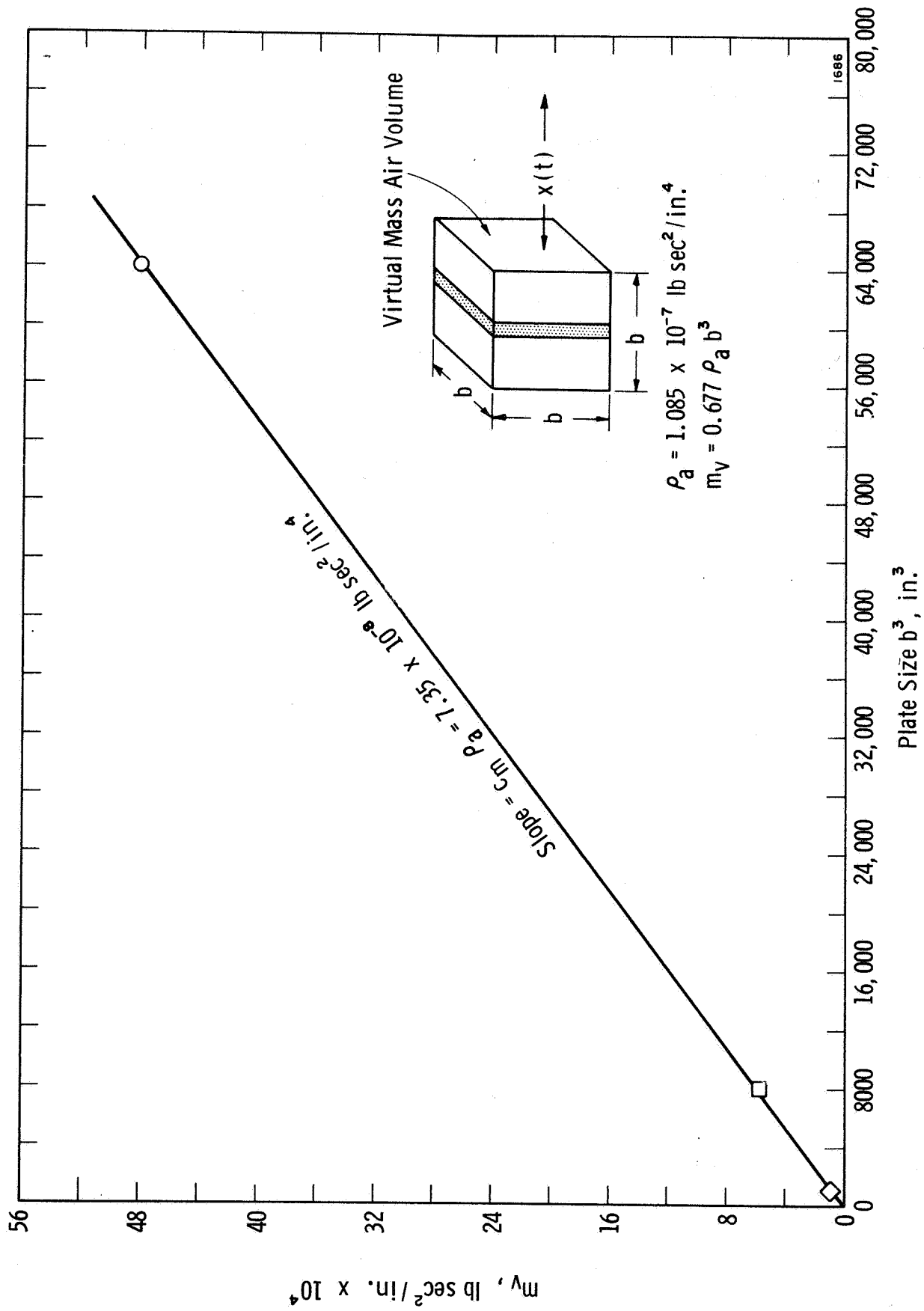


FIGURE 22. VIRTUAL MASS COEFFICIENTS OBTAINED FROM FREE-DECAY PERIOD CHANGES

and

$$\dot{y}(x, t) \approx A_n \omega_n \Phi_n(x) \cos \omega_n t \quad (27)$$

Then, it can be shown using an energy method (Ref. 11) that the logarithmic decrement as a result of air drag effects can be expressed as

$$\delta_a = \frac{4}{3} \left(\frac{\rho_a A_n S \tilde{C}_d}{m_b} \right) \beta_n \quad (28)$$

where β_n is the mode shape contribution factor with values shown in Table 2 for the first five cantilever beam modes.

TABLE 2. - MODE SHAPE CONTRIBUTION FACTORS
FOR THE FIRST FIVE MODES OF A THIN
CANTILEVER BEAM

n	β_n
1	1.473
2	1.300
3	1.270
4	1.252
5	1.252

In turn, it could be written that the successive amplitudes are

$$(A_n)_{i+1} = \left\{ \frac{(A_n)_i}{\left[1 + \frac{4}{3} \frac{\rho_a (A_n)_i S \tilde{C}_d \beta_n}{m_b} \right]} \right\} \quad i = 0, 1, 2, 3, \dots, \text{etc.} \quad (29)$$

as a result of the effects of air damping, and, providing the material damping can be expressed analytically, a similar equation can be determined which combines both the material and air damping. As an example of a typical solution for a combination of both quadratic damping and linear viscous damping, the reader is referred to page 195 of Reference 10.

CONCLUSIONS

An investigation has been conducted in order to determine oscillatory drag coefficients for rigid, two-dimensional plates oscillating normal to their planes. A dimensional analysis was conducted in order to establish possible parameters which might affect the oscillatory drag coefficients. Parameters which were investigated under the present program and were discussed in the report are amplitude, frequency, thickness, and area. In addition, the virtual mass effects were determined and discussed. Finally, a method was presented for an engineering application of the oscillatory drag coefficient data. Based on these studies, the following conclusions were made:

- (1) Within the range of period parameters chosen, the oscillatory drag coefficients were larger than drag coefficients obtained under steady flow conditions. The oscillatory drag coefficients for a particular plate were constant as a function of amplitude with the exception of very small amplitudes. At the small amplitudes, the analysis method becomes less accurate, and to discuss definite trends for these small amplitudes would be premature.
- (2) The oscillatory drag coefficients showed negligible variations, as a function of the frequency of the panel oscillations, i. e., at least in the range of 0.48 to 0.93 Hz. Based on the present study and the results of Stephens and Scavullo, it appears that the drag coefficients are independent of frequency in the frequency range of 0.48 to 21.2 Hz.
- (3) The drag coefficients presented in this report are a function of the surface area raised to the four-thirds power which is in agreement with the investigations of Stephens and Scavullo; however, the drag coefficients in the present investigations were only one-fifth as large as those of Stephens and Scavullo. This suggests that as of yet there exists an additional parameter(s) which has not been considered.
- (4) It was established that in general the panel width to thickness ratio has no effect on the oscillatory drag coefficient. There were some differences in the drag coefficients at the lower amplitudes; however, it should also be noted that the data were less reliable in this range.
- (5) An oscillatory mass coefficient of $\tilde{C}_m = 0.67$ was determined from the free-decay tests. This compares to a value of $\tilde{C}_m = 1.35$ obtained by Kuelegan and Carpenter at a slightly higher period parameter; however, the trend was for Kuelegan and Carpenter's

value of \tilde{C}_m to decrease with period parameter. Their plates had an infinite aspect ratio, whereas the present tests were conducted on plates with an aspect ratio of one.

- (6) It has been demonstrated that the values of \tilde{C}_d obtained experimentally on a rigid plate can be extended to a vibrating thin cantilever beam and provide useful engineering information.

SOUTHWEST RESEARCH INSTITUTE
Dept. of Mechanical Sciences
San Antonio, Texas, February 1968

REFERENCES

1. Baker, W. E.; and Allen, F. J.: The Damping of Transverse Vibrations of Thin Beams in Air. Ballistic Research Laboratories Report No. 1033, October 1957.
2. Stephens, David G.; and Scavullo, Maurice A.: Investigation of Air Damping of Circular and Rectangular Plates, a Cylinder and a Sphere. NASA TN D-1865, 1965.
3. Woolam, William E.; and Baker, W. E.: Drag on Flat Plates Oscillating Normal to Their Faces. Submitted for publication J. A. S. A.
4. Kuelegan, Garbis H.; and Carpenter, Lloyd H.: Forces on Cylinders and Plates in an Oscillating Fluid. Journal of Research of the National Bureau of Standards, vol. 60, no. 5, May 1958.
5. Martin, M.: Roll Damping Due to Bilge Keels. Ph. D. Thesis, State University of Iowa, 1959.
6. Ridjanovic, Muhamed: Drag Coefficients of Flat Plates Oscillating Normally to Their Planes. Schiffstechnik, Bd. 9, Heft 45, 1962.
7. Hoerner, Sighard F.: Fluid-Dynamic Drag. Second Ed., published by author, 1965, pp. 3-15.
8. Schwind, R. G.; Scotti, R. S.; and Skogh, J.: Analysis of Flexible Baffles for Damping Tank Sloshing. Journal of Spacecraft and Rockets, vol. 4, no. 1, pp. 47-53, January 1967.
9. Abramson, H. N., editor: The Dynamic Behavior of Liquids in Moving Containers. NASA SP-106, 1966.
10. Minorsky, N.: Introduction to Non-Linear Mechanics. First ed., J. W. Edwards, 1947.
11. Baker, W. E.; Woolam, William E.; and Young, Dana: Air and Internal Damping of Thin Cantilever Beams. International Journal of Mechanical Sciences, vol. 9, 1967, pp. 743-766.